รายงานวิจัยฉบับสมบูรณ์

โครงการ
การดัดแปลงยีสต์ *Saccharomyces cerevisiae* ให้สามารถใช้น้ำตาลไซโลสได้เพื่อการผลิตสารมูลค่าสูงจากชีวมวล

โดย ดร. วีรวัฒน์ รังกุพันธุ์ และ คณะ

1 พฤษภาคม พ.ศ. 2563

สัญญาเลขที่ TRG6180006

รายงานวิจัยฉบับสมบูรณ์

โครงการ การดัดแปลงยีสต์ *Saccharomyces cerevisiae* ให้สามารถใช้น้ำตาลไซโลสได้เพื่อการผลิตสารมูลค่าสูงจากชีวมวล

ดร. วีรวัฒน์ รังกุพันธุ์ และ คณะ
ศูนย์พันธุวิศวกรรมและเทคโนโลยีชีวภาพแห่งชาติ

สนับสนุนโดยสำนักงานกองทุนสนับสนุนการวิจัย
และต้นสังกัด

(ความเห็นในรายงานนี้เป็นของผู้วิจัย
สกว.และต้นสังกัดไม่จำเป็นต้องเห็นด้วยเสมอไป)

รูปแบบ Abstract (บทคัดย่อ)

Project Code:	**TRG6180006**
(รหัสโครงการ)	
Project Title:	Engineering Xylose Utilization in the Yeast *Saccharomyces cerevisiae* for Efficient Conversion of Biomass Hydrolysates to High Value Chemicals
(ชื่อโครงการ)	**การดัดแปลงยีสต์ *Saccharomyces cerevisiae* ให้สามารถใช้น้ำตาลไซโลสได้เพื่อการผลิตสารมูลค่าสูงจากชีวมวล**
Investigator:	**Dr. Weerawat Runguphan**
(ชื่อนักวิจัย)	**ดร. วีรวัฒน์ รังกุพันธุ์** **ศูนย์พันธุวิศวกรรมและเทคโนโลยีชีวภาพแห่งชาติ**
E-mail Address:	**Weerawat.run@biotec.or.th**
Project Period:	**2 ปี ตั้งแต่ วันที่ 2 พฤษภาคม พ.ศ. 2561 ถึง 1 พฤษภาคม พ.ศ. 2563**
(ระยะเวลาโครงการ)	

บทคัดย่อ

สภาวะโลกร้อนและปริมาณความต้องการของเชื้อเพลิงที่มากกว่ากำลังผลิต ทำให้หลายฝ่ายต่างให้ความสนใจในเชื้อเพลิงทดแทน โดยเฉพาะเชื้อเพลิงชีวภาพ ในช่วงหลายปีที่ผ่านมาการใช้ระบบจุลินทรีย์เพื่อผลิตเชื้อเพลิงพลังงานสูงผ่านกระบวนการทางชีวภาพ ได้กลายเป็นทางเลือกหนึ่งที่เป็นมิตรต่อสิ่งแวดล้อมและสามารถใช้งานได้จริงในระดับอุตสาหกรรม ยีสต์สายพันธุ์ *Saccharomyces cerevisiae* เป็นจุลินทรีย์ที่ได้รับความนิยมเป็นอย่างมากในการพัฒนาและดัดแปลงเพื่อผลิตเชื้อเพลิงชีวภาพที่หลากหลาย อย่างไรก็ตามข้อจำกัดที่สำคัญอย่างหนึ่งของ *S. cerevisiae* คือไม่สามารถใช้ไซโลสซึ่งเป็นน้ำตาลที่มีปริมาณมากที่สุดเป็นอันดับสองในชีวมวลลิกโนเซลลูโลส (lignocellulosic biomass) สำหรับการเจริญเติบโตและการผลิตสารเคมีได้ ดังนั้นการพัฒนาสายพันธุ์ *S. cerevisiae* ให้สามารถใช้ไซโลสได้อย่างมีประสิทธิภาพจึงมีความสำคัญอย่างยิ่ง

งานวิจัยนี้มุ่งมั่นพัฒนาเชื้อ *S. cerevisiae* ให้สามารถใช้ไซโลสเป็นแหล่งคาร์บอนได้อย่างมีประสิทธิภาพ ด้วยกระบวนการทางชีววิทยาศาสตร์สังเคราะห์ (synthetic biology) เราคัดกรองเอนไซม์ไซโลสรีดักเตส (xylose reductase, XR) และไซลิทอลดีไฮโดรจีเนส (xylitol dehydrogenase, XDH) จากยีสต์หลายสายพันธุ์ที่สามารถย่อยสลายไซโลสได้เองในธรรมชาติ เพื่อหาคู่เอนไซม์ XR-XDH ที่เหมาะสมและมีค่ากิจกรรมเอนไซม์ที่สูงที่สุดในยีสต์ *S. cerevisiae* เมื่อคัดกรองได้ดังกล่าว เราแสดงออกเอนไซม์ทั้งสองในยีสต์ *S. cerevisiae* ร่วมกับเอนไซม์ไซลูโลไคเนส (xylulokinase, XK) และเอนไซม์ทั้ง 5 เอนไซม์ในวิถีเมตาบอลิซึ่มของไอโซบิวทานอล อีกทั้งยังลดการแสดงออกของเอนไซม์ PHO13 และ GRE3 สายพันธุ์ดังกล่าว (เรียกว่า PWY2353) สามารถผลิตไอโซบิวทานอลได้ 48.4 ± 2.0 มิลลิกรัมต่อลิตร ต่อมาเราใช้เทคนิค adaptive laboratory evolution เพื่อให้ได้เชื้อกลายพันธุ์ (evolved mutant) ของเชื้อ PWY2353 ที่มีประสิทธิภาพในการใช้ไซโลสได้ดีขึ้น อีกทั้งยังมีอัตราการเติบโตที่สูงขึ้นกว่าเดิมด้วย จากการถอดรหัสพันธุกรรมในระดับจีโนมของเชื้อกลายพันธุ์ทำให้เราค้นพบการเปลี่ยนแปลงลำดับเบสในยีน 2 ยีนได้แก่ *CCR4* และ *TIF1* ที่ช่วยเพิ่มอัตราการเติบโตเฉพาะ (specific growth rate) ของยีสต์ 23% และ 14% ตามลำดับ นับว่าเป็นการค้นพบบทบาทหรือความเกี่ยวข้องของยีน *CCR4* และ *TIF1* ต่อความสามารถในการใช้ไซโลสของยีสต์ที่ไม่เคยมีการรายงานมาก่อน สุดท้ายเราทำการปรับระดับการแสดงออกของเอนไซม์คอขวด (fine-tuning bottle-neck enzyme) ในวิถีเมตาบอลิซึ่มของไอโซบิวทานอล เพื่อเพิ่มปริมาณการผลิต ไอโซบิวทานอล โดยสายพันธุ์ที่ดีที่สุดของเรา (PWY2353ev34b) สามารถผลิตไอโซบิวทานอลได้ 92.9 ± 4.4 มิลลิกรัมต่อลิตร ซึ่งสูงกว่าปริมาณการผลิตของสายพันธุ์ที่มีการรายงานก่อนหน้านี้ถึง 68 เท่า (สายพันธุ์ Isoy16, 1.36 มิลลิกรัมต่อลิตร) เราหวังว่างานวิจัยของเราจะสามารถนำไปขยายขนาดและพัฒนาเป็นเป็นกระบวนการ ผลิตไอโซบิวทานอลและสารมีค่าอื่นๆจากไซโลสในระดับอุตสาหกรรมต่อไป

Abstract

As the importance of reducing carbon emissions as a means to limit the serious effects of global climate change becomes apparent, synthetic biologists and metabolic engineers are looking to develop renewable sources for transportation fuels and petroleum-derived chemicals. In recent years, microbial production of high-energy fuels has emerged as an attractive alternative to the traditional production of transportation fuels. In particular, the Baker's yeast *Saccharomyces cerevisiae*, a highly versatile microbial chassis, has been engineered to produce a wide array of biofuels. Nevertheless, a key limitation of *S. cerevisiae* is its inability to utilize xylose, the second most abundant sugar in lignocellulosic biomass, for both growth and chemical production. Therefore, the development of a robust *S. cerevisiae* strain that is able to use xylose is of great importance.

Here, we engineered *S. cerevisiae* to efficiently utilize xylose as a carbon source and produce the advanced biofuel isobutanol. Specifically, we screened xylose reductase (XR) and xylose dehydrogenase (XDH) variants from different xylose-metabolizing yeast strains to identify the XR–XDH combination with the highest activity. Overexpression of the selected XR–XDH variants, a xylose-specific sugar transporter, xylulokinase, and isobutanol pathway enzymes in conjunction with the deletions of *PHO13* and *GRE3* resulted in an engineered strain (PWY2353) that is capable of producing isobutanol at a titer of 48.4 ± 2.0 mg/L. Next, we subjected PWY2353 to adaptive laboratory evolution to further improve the strain's ability to utilize xylose. Whole genome resequencing of several evolved strains followed by reverse engineering identified two single nucleotide mutations, one in *CCR4* and another in *TIF1*, that improved the yeast's specific growth rate by 23% and 14%, respectively. Neither one of these genes has previously been implicated to play a role in utilization of D-xylose. Finally, we fine-tuned the expression levels of the bottleneck enzymes in the isobutanol pathway to improve the evolved strain's isobutanol titer to 92.9 ± 4.4 mg/L (specific isobutanol production of 50.2 ± 2.6 mg/g CDW), a 90% improvement in titer and a 110% improvement in specific production over the non-evolved strain. We hope that our work will set the stage for an economic route to the advanced biofuel isobutanol and enable efficient utilization of xylose-containing biomass.

1. Introduction

Concerns over global warming and unsustainable demands have increased interest in renewable fuels and chemicals. Microbial production of biofuels using cost-competitive and environmentally friendly bioprocesses is a viable alternative to the traditional production of transportation fuels [1–3]. Notable examples of microbially produced biofuels include branched-chain and higher alcohols as gasoline replacements and fatty acid ethyl ester (FAEE) and long-chain alkanes as diesel replacements [4–10]. In many of these examples, the Budding yeast *S. cerevisiae* was the host of choice because of its ideal properties as a chemical production platform. These properties include: i) high tolerance to many industrial stresses, including low pH and high osmotic pressure; ii) high tolerance to the biofuel compound of interest and contaminants from the pretreatment steps; iii) availability of "omics" data and genetic tools for bottom-up strain engineering; iv) resistance to phage infection. A major drawback of *S. cerevisiae*, however, is its inability to utilize D-xylose, a five-carbon (C5) sugar that is the second most abundant sugar in lignocellulosic biomass (~30%–40%), as a carbon source [11].

Increasingly, the use of starch or the sucrose fractions of agricultural crops as the carbon substrates for biomass conversion has become less attractive due to environmental, economical and ethical considerations [12]. Instead, lignocellulosic biomass, such as agricultural residues and energy crops, offers a cheap and renewable alternative carbon source for the microbial production of biofuels. Since xylose is the second most abundant component of lignocellulosic biomass, enabling the yeast *S. cerevisiae* to efficiently utilize xylose and convert it into biofuels is of great importance and has been the focus of intense and highly competitive research [13]. An extensive body of work has resulted in engineered strains that are capable of producing near-theoretical yields of ethanol from pure xylose and xylose-containing biomass [14]. To create such a strain, a xylose assimilation pathway is introduced into *S. cerevisiae*, enabling the resulting strain to convert xylose into xylulose and then xylulose-5-phosphate, a starting metabolite to the non-oxidative Pentose Phosphate Pathway (PPP) (**Figure 1**) [15]. The

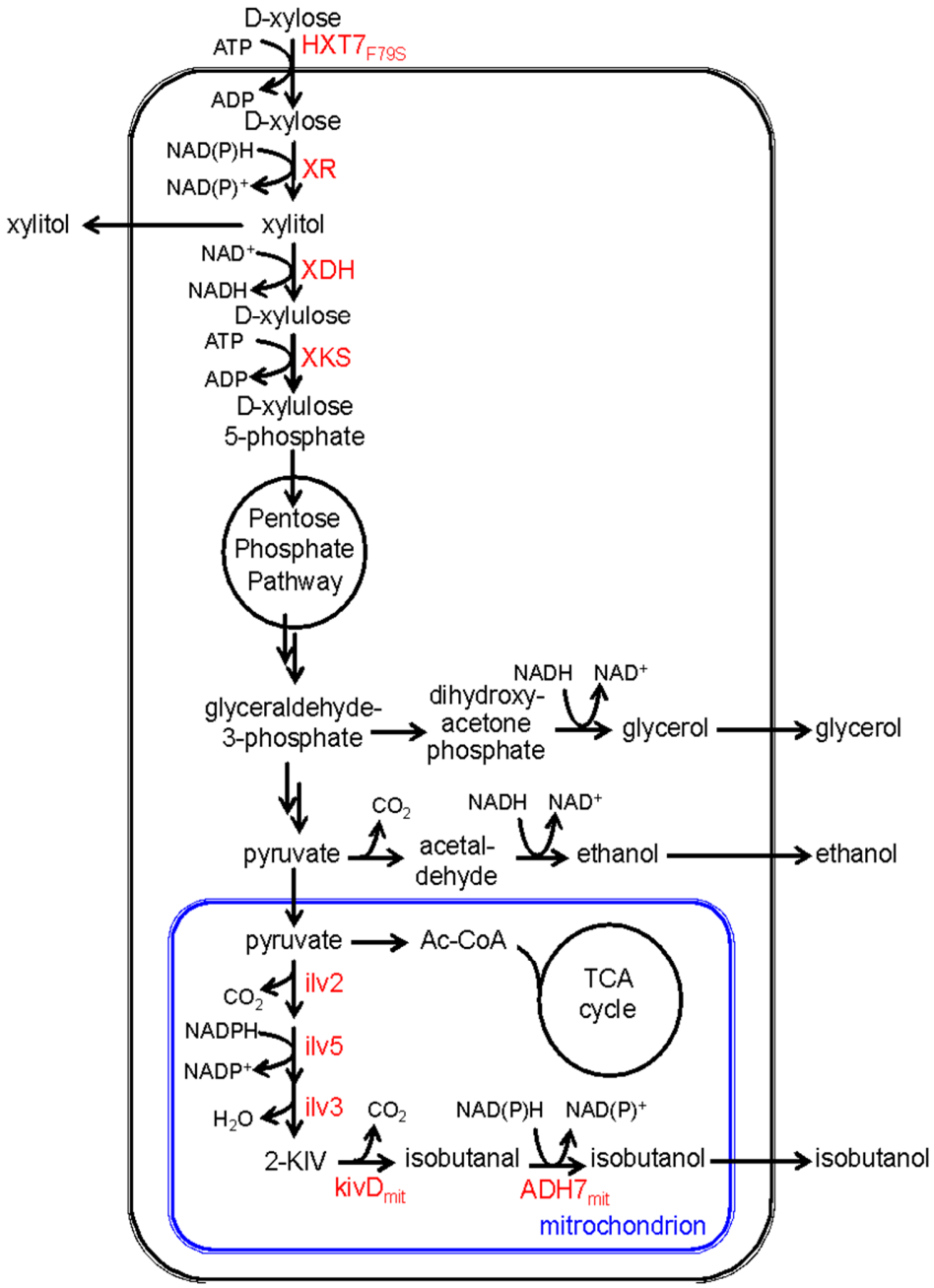

Figure 1. Engineered isobutanol production from D-xylose in *S. cerevisiae*. *$HXT7_{F79S}$* high affinity glucose transporter with a *F79S* point mutation, *XR* xylose reductase, *XDH* xylitol dehydrogenase, *XKS* xylulokinase, *Ilv2* acetolactate synthase, *Ilv5* acetohydroxyacid reductoisomerase, *Ilv3* dihydroxyacid dehydratase, *kivDmit* mitochondrially-targeted keto-acid decarboxylase, *ADH7mit* mitochondrially-targeted alcohol dehydrogenase. Enzymes highlighted in red are overexpressed.

two products of the PPP, glyceraldehyde-3-phosphate and fructose-6-phosphate, then enter glycolysis, producing pyruvate and leading to ethanol production.

Two distinct pathways exist in xylose-fermenting organisms for the conversion of xylose to xylulose: the xylose reductase-xylitol dehydrogenase (XR-XDH) pathway in yeast and aerobic fungal species and the xylose isomerase (XI) pathway in bacteria and anaerobic fungal [11]. In the XR-XDH pathway, XR first reduces xylose to xylitol using NADPH and/or NADH as a cofactor. XDH then converts xylitol into xylulose with a specific cofactor preference for NAD^+. Because of the dual cofactor preference, the redox imbalance hinders successful implementation of the XR-XDH pathway. Conversely, in the XI pathway, XI converts xylose to xylulose without requiring any cofactor. However, as XI enzymes tend to have lower catalytic efficiency compared to XR-XDH enzymes, they are less attractive for industrial-scale applications.

Although microbial ethanol fermentation has played an important role in the transition from conventional fossil fuels to bio-based fuels, ethanol is not an ideal gasoline replacement due to its poor physicochemical properties [16]. Specifically, ethanol has low energy density (~ 70% of the energy content of gasoline), high tendency to absorb water, and high vapor pressure. In contrast, higher and branched-chain alcohols, such as butanol and isobutanol, have superior energy density and are more compatible with the existing distribution and storage infrastructures [17]. Moreover, branched-chain alcohols have higher octane numbers compared with their straight-chain counterparts and are therefore ideal gasoline substitutes for high performance petrol engines.

To produce branched-chain and higher alcohols in a non-native producer, Atsumi and coworkers devised a strategy which involves “hijacking” the native amino acid metabolism of the host organism and diverts the amino acid intermediate to the 2-keto acid degradation pathway for higher alcohol production [5]. In the L-valine biosynthetic pathway, acetolactate synthase (Ilv2) condenses two molecules of pyruvate to 2-acetolactate, which is then reduced to 2,3-dihydroxyisovalerate by acetohydroxyacid reductoisomerase (Ilv5). Next, 2,3-dihydroxyisovalerate is converted to 2-ketoisovalerate, a key intermediate in L-valine biosynthesis, by dihydroxyacid

dehydratase (Ilv3). In the ketoacid degradation pathway, 2-ketoisovalerate is converted to isobutanal by introducing a heterologous ketoacid decarboxylase (kivD) from the bacterium *Lactococcus lactis* or by overexpression of the endogenous decarboxylase (Aro10). The resulting aldehyde is then reduced by an alcohol dehydrogenase (Adh7 or Adh2) from *S. cerevisiae* to the final alcohol products, including isobutanol. Though the original work was done in *E. coli*, several labs have since applied this strategy to produce isobutanol in many organisms including the cyanobacterium *Synechococcus elongatus* PCC7942, the soil bacterium *Ralstonia eutropha*, and more recently, the methylotrophic yeast *Pichia pastoris* [18–20].

While production of isobutanol from glucose in the yeast system is well established, we found only one previous report of branched-chain alcohol production from xylose in *S. cerevisiae* [21]. In the study, Brat and Boles overexpressed the xylose isomerase XylA from *Clostridium phytofermentans* along with isobutanol pathway enzymes in *S. cerevisiae*. The engineered strain produced isobutanol at a yield of 0.16 mg/g xylose, well below the reported yields from glucose of up to 16 mg/g glucose [22].

Here, we improved upon this previous work and engineered an efficient isobutanol producing strain of *S. cerevisiae*. Specifically, we first screened XR-XDH pathway genes from various xylose-utilizing species to identify an optimal XR-XDH gene combination. Second, we integrated the isobutanol pathway, which comprises the first portion of the endogenous L-valine biosynthesis and keto-acid degradation pathway. Third, we disrupted two endogenous genes that have previously been shown to improve xylose assimilation in *S. cerevisiae*. Fourth, we used adaptive laboratory evolution to improve our engineered yeast strain's ability to utilize D-xylose. We used whole genome resequencing and reverse engineering to verify the roles of SNPs in improving growth on xylose. Finally, we fine-tuned the expression level of the each gene in the xylose utilization pathway and isobutanol pathway. We envision that our yeast platform will pave the way for a scalable and economic route to the production of biofuels utilizing environmentally sensitive and less carbon-intensive agricultural wastes and energy crops.

Table 1. Strains generated in this study

Strain name	Genotype	Description	Reference
BY4742	*Mat α; his3Δ1; leu2Δ0; lys2Δ0; ura3Δ0*	Lab strain	Lab strain
PWY1113	*Mat α; his3Δ1; leu2Δ0; lys2Δ0; ura3Δ0; ARS208:: P_{TEF1}-SsXKS; YMRWΔ15:: P_{TEF1}-HXTF79S; ARS308:: P_{TEF1}-CtXYL1; ARS720:: P_{TEF1}-CtXYL2*	BY4742 overexpressing *XKS* from *Scheffersomyces stipitis*, *HXT7*_F79S from *Saccharomyces cerevisiae*, *XYL1* from *Candida tropicalis* and *XYL2* from *Candida tropicalis*	This study
PWY1213	*Mat α; his3Δ1; leu2Δ0; lys2Δ0; ura3Δ0; ARS208:: P_{TEF1}-SsXKS; YMRWΔ15:: P_{TEF1}-HXTF79S; ARS308:: P_{TEF1}-CsXYL1; ARS720:: P_{TEF1}-CtXYL2*	BY4742 overexpressing *XKS* from *Scheffersomyces stipitis*, *HXT7*_F79S from *Saccharomyces cerevisiae*, *XYL1* from *Candida shehatae* and *XYL2* from *Candida tropicalis*	This study
PWY1313	*Mat α; his3Δ1; leu2Δ0; lys2Δ0; ura3Δ0; ARS208:: P_{TEF1}-SsXKS; YMRWΔ15:: P_{TEF1}-HXTF79S; ARS308:: P_{TEF1}-SsXYL1; ARS720:: P_{TEF1}-CtXYL2*	BY4742 overexpressing *XKS* from *Scheffersomyces stipitis*, *HXT7*_F79S from *Saccharomyces cerevisiae*, *XYL1* from *Scheffersomyces stipitis* and *XYL2* from *Candida tropicalis*	This study
PWY1413	*Mat α; his3Δ1; leu2Δ0; lys2Δ0; ura3Δ0; ARS208:: P_{TEF1}-SsXKS; YMRWΔ15:: P_{TEF1}-HXTF79S; ARS308:: P_{TEF1}-SpXYL1.1; ARS720:: P_{TEF1}-CtXYL2*	BY4742 overexpressing *XKS* from *Scheffersomyces stipitis*, *HXT7*_F79S from *Saccharomyces cerevisiae*, *XYL1.1* from *Spathaspora passalidarum* and *XYL2* from *Candida tropicalis*	This study
PWY1513	*Mat α; his3Δ1; leu2Δ0; lys2Δ0; ura3Δ0; ARS208:: P_{TEF1}-SsXKS; YMRWΔ15:: P_{TEF1}-HXTF79S; ARS308:: P_{TEF1}-SpXYL1.2; ARS720:: P_{TEF1}-*	BY4742 overexpressing *XKS* from *Scheffersomyces stipitis*, *HXT7*_F79S from *Saccharomyces cerevisiae*, *XYL1.2* from *Spathaspora*	This study

	CtXYL2	*passalidarum* and *XYL2* from *Candida tropicalis*	
PWY2113	*Mat α; his3Δ1; leu2Δ0; lys2Δ0; ura3Δ0; ARS208:: P_{TEF1}-SsXKS; YMRWΔ15:: P_{TEF1}-HXTF79S; ARS308:: P_{TEF1}-CtXYL1; ARS720:: P_{TEF1}-SsXYL2*	BY4742 overexpressing *XKS* from *Scheffersomyces stipitis*, *HXT7*_F79S from *Saccharomyces cerevisiae*, *XYL1* from *Candida tropicalis* and *XYL2* from *Scheffersomyces stipitis*	This study
PWY2213	*Mat α; his3Δ1; leu2Δ0; lys2Δ0; ura3Δ0; ARS208:: P_{TEF1}-SsXKS; YMRWΔ15:: P_{TEF1}-HXTF79S; ARS308:: P_{TEF1}-CsXYL1; ARS720:: P_{TEF1}-SsXYL2*	BY4742 overexpressing XKS from *Scheffersomyces stipitis*, *HXT7*_F79S from *Saccharomyces cerevisiae*, *XYL1* from *Candida shehatae* and *XYL2* from *Scheffersomyces stipitis*	This study
PWY2313	*Mat α; his3Δ1; leu2Δ0; lys2Δ0; ura3Δ0; ARS208:: P_{TEF1}-SsXKS; YMRWΔ15:: P_{TEF1}-HXTF79S; ARS308:: P_{TEF1}-SsXYL1; ARS720:: P_{TEF1}-SsXYL2*	BY4742 overexpressing *XKS* from *Scheffersomyces stipitis*, *HXT7*_F79S from *Saccharomyces cerevisiae*, *XYL1* from *Scheffersomyces stipitis* and *XYL2* from *Scheffersomyces stipitis*	This study
PWY2413	*Mat α; his3Δ1; leu2Δ0; lys2Δ0; ura3Δ0; ARS208:: P_{TEF1}-SsXKS; YMRWΔ15:: P_{TEF1}-HXTF79S; ARS308:: P_{TEF1}-SpXYL1.1; ARS720:: P_{TEF1}-SsXYL2*	BY4742 overexpressing *XKS* from *Scheffersomyces stipitis*, *HXT7*_F79S from *Saccharomyces cerevisiae*, *XYL1.1* from *Spathaspora passalidarum* and *XYL2* from *Scheffersomyces stipitis*	This study
PWY2513	*Mat α; his3Δ1; leu2Δ0; lys2Δ0; ura3Δ0; ARS208:: P_{TEF1}-SsXKS; YMRWΔ15:: P_{TEF1}-HXTF79S; ARS308:: P_{TEF1}-SpXYL1.2; ARS720:: P_{TEF1}-SsXYL2*	BY4742 overexpressing *XKS* from *Scheffersomyces stipitis*, *HXT7*_F79S from *Saccharomyces cerevisiae*, *XYL1.2* from *Spathaspora passalidarum* and *XYL2* from *Scheffersomyces stipitis*	This study
PWY3113	*Mat α; his3Δ1; leu2Δ0; lys2Δ0;*	BY4742 overexpressing XKS from	This study

	ura3Δ0; ARS208:: P_{TEF1}-SsXKS; YMRWΔ15:: P_{TEF1}-HXTF79S; ARS308:: P_{TEF1}-CtXYL1; ARS720:: P_{TEF1}-SpXYL2	*Scheffersomyces stipitis*, *HXT7*_F79S from *Saccharomyces cerevisiae*, *XYL1* from *Candida tropicalis* and *XYL2* from *Spathaspora passalidarum*	
PWY3313	*Mat α; his3Δ1; leu2Δ0; lys2Δ0; ura3Δ0; ARS208:: P_{TEF1}-SsXKS; YMRWΔ15:: P_{TEF1}-HXTF79S; ARS308:: P_{TEF1}-SsXYL1; ARS720:: P_{TEF1}-SpXYL2*	BY4742 overexpressing *XKS* from *Scheffersomyces stipitis*, *HXT7*_F79S from *Saccharomyces cerevisiae*, *XYL1* from *Scheffersomyces stipitis* and *XYL2* from *Spathaspora passalidarum*	This study
PWY3413	*Mat α; his3Δ1; leu2Δ0; lys2Δ0; ura3Δ0; ARS208:: PTEF1-SsXKS; YMRWΔ15:: PTEF1-HXTF79S; ARS308:: PTEF1-SpXYL1.1; ARS720:: PTEF1-SpXYL2*	BY4742 overexpressing *XKS* from *Scheffersomyces stipitis*, *HXT7*_F79S from *Saccharomyces cerevisiae*, *XYL1.1* from *Spathaspora passalidarum* and *XYL2* from *Spathaspora passalidarum*	This study
PWY3513	*Mat α; his3Δ1; leu2Δ0; lys2Δ0; ura3Δ0; ARS208:: P_{TEF1}-SsXKS; YMRWΔ15:: P_{TEF1}-HXTF79S; ARS308:: P_{TEF1}-SpXYL1.2; ARS720:: P_{TEF1}-SpXYL2*	BY4742 overexpressing *XKS* from *Scheffersomyces stipitis*, *HXT7_F79S* from *Saccharomyces cerevisiae*, *XYL1.2* from *Spathaspora passalidarum* and *XYL2* from *Spathaspora passalidarum*	This study
PWY1123	PWY1113 *GRE3Δ*	PWY1113 *GRE3* deleted	This study
PWY1223	PWY1213 *GRE3Δ*	PWY1213 *GRE3* deleted	This study
PWY2323	PWY2313 *GRE3Δ*	PWY2313 *GRE3* deleted	This study
PWY3323	PWY3313 *GRE3Δ*	PWY3313 *GRE3* deleted	This study
PWY1133	PWY1123 *YORW Δ22:: P_{TDH3} – LlkivDmt-T2A-ScADH7mt*	PWY1123 overexpressing *ADH7* from *Saccharomyces cerevisiae* and *kivD* from *Lactococcus lactis*	This study

PWY1143	PWY1133 *ARS1309:: P_{TEF1}-ScIlv2-T2A-ScIlv5-T2A-ScIlv3*	PWY1133 overexpressing *Ilv2, Ilv5, Ilv3* from *Saccharomyces cerevisiae*	This study
PWY1153	PWY1143 *PHO13Δ*	PWY1143 *PHO13* deleted	This study
PWY2333	PWY2323 *YORW Δ22:: PTDH3 – LlkivDmt-T2A-ScADH7mt*	PWY2323 overexpressing *ADH7* from *Saccharomyces cerevisiae* and *kivD* from *Lactococcus lactis*	This study
PWY2343	PWY2333 *ARS1309:: P_{TEF1}-ScIlv2-T2A-ScIlv5-T2A-ScIlv3*	PWY2333 overexpressing *Ilv2, Ilv5, Ilv3* from *Saccharomyces cerevisiae*	This study
PWY2353	PWY2343 *PHO13Δ*	PWY2343 *PHO13* deleted	This study
PWY2353ev 17	PWY2353; adaptive laboratory evolution clone No. 17	PWY2353 subjected to adaptive laboratory evolution, clone No. 17	This study
PWY2353ev 34	PWY2353; adaptive laboratory evolution clone No. 34	PWY2353 subjected to adaptive laboratory evolution, clone No. 34	This study
PWY2353ev 36	PWY2353; adaptive laboratory evolution clone No. 36	PWY2353 subjected to adaptive laboratory evolution, clone No. 36	This study
PWY2353ev 38	PWY2353; adaptive laboratory evolution clone No. 38	PWY2353 subjected to adaptive laboratory evolution, clone No. 38	This study
PWY2363	PWY2353 *ARS416:: P_{TDH3} –LlkivDmt-T2A-ScADH7mt*	PWY2353 overexpressing one extra copy each of *ADH7* from *S. cerevisiae* and *kivD* from *L. lactis*	This study
PWY2373	PWY2353 *ARS416:: P_{TDH3} –LlkivDmt-T2A-ScADH7mt; ARS1014:: P_{TEF1}-ScIlv2-T2A-ScIlv5-T2A-ScIlv3*	PWY2353 overexpressing one extra copy each of *Ilv2, Ilv5, Ilv3, ADH7* from *S. cerevisiae* and *kivD* from *L. lactis*	This study
PWY2353ev 34a	PWY2353ev34 *ARS416:: P_{TDH3} – LlkivDmt-T2A-ScADH7mt*	PWY2353ev34 overexpressing one extra copy each of *ADH7* from *S. cerevisiae* and *kivD* from *L. lactis*	This study
PWY2353ev	PWY2353ev34 *ARS416:: P_{TDH3} –*	PWY2353ev34 overexpressing one extra copy	This study

34b	*LlkivDmt-T2A-ScADH7mt; ARS1014::* P_{TEF1}*-ScIlv2-T2A-ScIlv5-T2A-ScIlv3*	each of *Ilv2, Ilv5, Ilv3, ADH7* from *S. cerevisiae* and *kivD* from *L. lactis*	
PWY2383	PWY2353 *CCR4::CCR4*$_{A638S}$	PWY2353 whereby G at position 1912 of *CCR4* is mutated to T resulting in the amino acid change Ala638Ser	This study
PWY2393	PWY2353 *CCR4::CCR4*$_{A638S}$*; TIF1::TIF1*$_{A79S}$	PWY2353 whereby G at position 1912 of *CCR4* is mutated to T resulting in the amino acid change Ala638Ser and G at position 235 of *TIF1* is mutated to T resulting amino acid change Ala79Ser	This study

Table 2. Plasmids generated in this study

Plasmid name	Overexpressed gene(s)	Promoter used for overexpression	Plasmid origin of replication	Selectable marker	Reference
pRSII416-SsXKS	*XKS* from *S. stipitis*	*TEF1*	CEN6/ARS4	Ura3	This study
pRSII416-SsXR	*XYL1* from *S. stipitis*	*TEF1*	CEN6/ARS4	Ura3	This study
pRSII416-SsXDH	*XYL2* from *S. stipitis*	*TEF1*	CEN6/ARS4	Ura3	This study
pRSII416-ScHXT7mut	*HXT7F79S* from *S. cerevisiae*	*TEF1*	CEN6/ARS4	Ura3	This study
pRSII416-LlkivD-T2A-ScADH7	*LlkivD*_mito from *Lactococcus lactis*, *ADH7* from *S. cerevisiae*	*TEF1*	CEN6/ARS4	Ura3	This study
pRSII416-ScIlv2-T2A-ScIlv5-T2A-ScIlv3	*Ilv2*, *Ilv5* and *Ilv3* from *S. cerevisiae*	*TEF1*	CEN6/ARS4	Ura3	This study
pRSII426-SsXKS	*XKS* from *S. stipitis*	*TEF1*	2μ	Ura3	This study
pRSII426-SsXR	*XYL1* from *S. stipitis*	*TEF1*	2μ	Ura3	This study

pRSII426-SsXDH	*XYL2* from *S. stipitis*	*TEF1*	2μ	Ura3	This study
pRSII426-ScHXT7mut	*HXT7F79S* from *S. cerevisiae*	*TEF1*	2μ	Ura3	This study
pRSII426-LlkivD-T2A-ScADH7	*LlkivD*_mito from *Lactococcus lactis*, *ADH7* from *S. cerevisiae*	*TEF1*	2μ	Ura3	This study

Table 3. Overview of different microbial strains engineered to produce isobutanol (specific growth rates and isobutanol titer) including those that were generated in this study

Strain name	Specific growth rate in glucose (h^{-1})	Specific growth rate in xylose (h^{-1})	Isobutanol titer in glucose (mg/L)[A]	Isobutanol titer in xylose (mg/L)[A]	Reference
Isoy16*	Not reported	Not reported	Not reported	1.36 ±0.11[B]	[21]
BY4742	0.1395 ±0.0003	N.D.	4.0 ±0.5	N.D.	This study
PWY0013	0.1329 ±0.0001	N.D.	5.5 ±0.7	N.D.	This study
PWY1113	0.1435 ±0.0004	0.0313±0.0011	2.8±0.1	3.8 ±0.4	This study
PWY2313	0.1461 ±0.0003	0.0423 ±0.0004	5.0±0.4	4.3 ±0.7	This study
PWY1123	0.1472 ±0.0003	0.0295 ±0.0012	13.9 ±0.9	5.7 ±0.6	This study
PWY2323	0.1436 ±0.0002	0.0426 ±0.0001	23.5 ±0.7	4.4 ±0.4	This study
PWY1143	0.1463 ±0.0003	0.0368 ±0.0015	30.4 ±1.0	9.4 ±0.3	This study
PWY2343	0.1476 ±0.0004	0.0431 ±0.0004	43.3 ±1.0	16.9 ±1.9	This study
PWY1153	0.1408 ±0.0003	0.0513 ±0.0002	33.9±1.2	11.8 ±0.8	This study
PWY2353	0.1469 ±0.0003	0.0532 ±0.0004	43.0 ±0.9	19.7 ±2.4	This study

* CEN.PK with deletions in *Ilv2, Ilv5* and *Ilv3* overexpressing XylA from *C. phytofermentans*, *XKS1* and *Aro10* from *S. cerevisiae* and cytosol-targeted *Ilv2*, *Ilv5* and *Ilv3* from *S. cerevisiae*

[A.] Isobutanol titers after 2 days of cultivation in yeast minimal medium

[B.] Isobutanol titers after 6 days of cultivation in yeast minimal medium

2. Materials and Method

2.1 Yeast strain, media and transformation

The yeast strains used in this study were constructed from BY4742 (derivative of S288C (*Mat* α*; his3*Δ*1; leu2*Δ*0; lys2*Δ*0; ura3*Δ*0*)) (**Table 1**). The plasmids used in this study were generated from the pRS416, pRSII416 and pRSII426 vector series (**Table 2**) [23]. pRS416 and pRSII416 contain the yeast CEN6/ARS4 origin of replication, which results in transformants with a low copy plasmid number (1 copy per cell). In contrast, pRSII426 contains the yeast 2μ origin of replication, which allows autonomous replication of the plasmids and results in transformants with a high plasmid copy number (10–40 copies per cell) [24]. The CRISPR-Cas9 plasmids used in this study for genome editing were generated from pRPR1-gRNA handle-RPR1t [25] and p414-TEF1p-Cas9-CYC1t [26].

Yeast and bacterial strains were stored in 25% glycerol at −80°C. *E. coli* was grown in Luria-Bertani medium. Ampicillin at 100 μg/ml was added to the medium when required. Yeast strain without plasmid was cultivated in YPD medium (10 g/L yeast extract, 20 g/L Bacto Peptone and 20 g/L glucose). Selection of yeast transformants with URA3 was done on a yeast selective medium (6.7 g/L of Yeast Nitrogen Base (Difco), 20 g/L glucose, and a mixture of appropriate nucleotide bases and amino acids with Uracil dropouts (CSM-URA). Yeast cells were cultivated at 30°C in 50 mL Falcon tubes or 250 mL Erlenmeyer flasks closed with cotton plug and shaken at 250 rpm.

XR and XH candidate genes were amplified from genomic DNA (in the cases where the strains are available in the Thailand Bioresource Research Center (TBRC)) or synthesized by Genscript. The individual genes were placed behind the P_{TEF1} promoter and separately integrated into the yeast genome at specific targets [27]. Gene knockouts were generated using a previously reported gene disruption cassette in *S. cerevisiae* [28]. Gene disruption cassettes containing the URA3 selectable marker flanked by loxP sites (obtained by PCR of the pUG72 plasmid) were produced with 42 base pairs of homology on either side of each target integration site. Oligonucleotide primers used

for PCR, cloning, chromosomal integration and gene knock-outs in this study are included in the **Supplementary Information**. Yeast cells were transformed using the LiAc/SS carrier DNA/PEG method as previously described [29, 30]. Following yeast transformations, colonies were selected on selective medium lacking uracil and confimed via PCR. The marker gene (URA3) was removed by overexpressing the Cre recombinase to excise the selection marker between the loxP sites in the disruption cassette. This enables subsequent rounds of genomic integrations. Cre recombinase was expressed using the inducible GAL1 promoter on plasmid pSH62 [31]. The strain harboring pSH62 was grown in SD medium plus 1 g/L 5-fluoroorotic acid to encourage loss of the URA3 [32]. To verify the genetic stability of the engineered strains, their genomic DNA was isolated (Promega Wizard Genomic DNA Purification kit) and then subjected to a diagnostic PCR amplification that amplified regions both upstream and downstream of the integration/deletion sites.

2.2 Plasmid construction

Plasmid pRS416Tef1-SsXKS: XKS (accession number: XM_001387288) was amplified from *S. stipitis* BCC47637 genomic DNA using primers S1 and S2. The SsXKS amplicon was ligated to the *Bam*HI/*Eco*RI site of p416Tef1-Ura3 [9] to yield pRS416Tef1-SsXKS.

Plasmid pRS416Tef1-HXT7_F79S: HXT7_F79S (accession number: NM_001180650) was amplified from *S. cerevisie* BY4742 genomic DNA as two fragments using primers S3 and S4, and S5 and S6. S4 and S5 primers contain the point mutation required for the amino acid substitution. The two fragments were placed behind the P_{TEF1} promoter in p416Tef1-Ura3 to form pRS416Tef1-HXT7_F79S using homologous recombination in yeast.

Plasmid pRS416Tef1-CtXYL1: CtXYL1 (accession number: MF045434) was amplified from *C. tropicalis* BCC59435 genomic DNA using primers S7 and S8. The CtXYL1 amplicon was ligated to the *Bam*HI/*Eco*RI site of p416Tef1-Ura3 to yield pRS416Tef1-CtXYL1.

Plasmid pRS416Tef1-CsXYL1: CsXYL1 (accession number: MN200231) was synthesized by Genscript and was ligated into the *Bam*HI/*Eco*RI site of p416Tef1-Ura3 to yield pRS416Tef1-CsXYL1.

Plasmid pRS416Tef1-SsXYL1: SsXYL1 (accession number: HM769331) was amplified from *S. stipitis* BCC47637 genomic DNA using primers S9 and S10. The SsXYL1 amplicon was ligated to the *Bam*HI/*Sma*I site of p416Tef1-Ura3 to yield pRS416Tef1-SsXYL1.

Plasmid pRS416Tef1-SpXYL1.1: SpXYL1.1 (accession number: MN200233) was synthesized by Genscript and was ligated into the *Bam*HI/*Eco*RI site of p416Tef1-Ura3 to yield pRS416Tef1-SpXYL1.1.

Plasmid pRS416Tef1-SpXYL1.2: SpXYL1.2 (accession number: MN200234) was synthesized by Genscript and was ligated into the *Bam*HI/*Eco*RI site of p416Tef1-Ura3 to yield pRS416Tef1-SpXYL1.2.

Plasmid pRS416Tef1-CtXYL2: CtXYL2 (accession number: JN631039) was amplified from *C. tropicalis* BCC59435 genomic DNA using primers S11 and S12. The CtXYL2 amplicon was ligated to the *Sac*II/*Eco*RI site of p416Tef1-Ura3 to yield pRS416Tef1-CtXYL2.

Plasmid pRS416Tef1-SsXYL2: SsXYL2 (accession number: HM769332) was amplified from *S. stipitis* BCC47637 genomic DNA using primers S13 and S14. The SsXYL2 amplicon was ligated to the *Sac*II/*Eco*RI site of p416Tef1-Ura3 to yield pRS416Tef1-SsXYL2.

Plasmid pRS416Tef1-SpXYL2: SpXYL2 (accession number: MN200232) was synthesized by Genscript and was ligated into the *Sac*II/*Eco*RI site of p416Tef1-Ura3 to yield pRS416Tef1-SpXYL2.

Plasmid pUG72-TDH3-LlkivDmit-2A-ScADH7mit: P_{TDH3} promoter (accession number: NM_00118132) and ADH7 (accession number: NM_001178812) were amplified from *S. cerevisie* BY4742 genomic DNA using primers S15 and S16, and S17 and S18, respectively. LlkivD (codon-optimized for *S. cerevisiae* expression; accession number: MN200235) was synthesized by Genscript and provided in pUC57 vector. The gene was amplified from pUC57-LlkivD using primers S19 and S20. The three amplicons (P_{TDH3}, LlkivD, ADH7) were joined together with pUG72 to form pUG72-TDH3-LlkivD-2A-

ScADH7. To add the mitochondria signal peptide sequence to LlkivD and ADH7, P_{TDH3}, LlkivD, ADH7 amplified from pUG72-TDH3-LlkivD-2A-ScADH7 using primer S15 and S21, S22 and S23, and S24 and S18, respectively. The three amplicons (P_{TDH3}, LlkivDmit, ADH7mit) were joined together with pUG72 to form pUG72-TDH3-LlkivDmit-2A-ScADH7mit.

Plasmid pRS416Tef1-ScIlv2-2A-ScIlv5-2A-ScIlv3: Ilv2 (accession number: NM_001182608), Ilv5 (accession number: NM_001182244) and Ilv3 (accession number: NM_001181674) were amplified from *S. cerevisie* BY4742 genomic DNA using primers S25 and S26, S27 and S28, and S29 and S30, respectively. The three amplicons were placed behind the P_{TEF1} promoter in p416Tef1-Ura3 to form pRS416Tef1-ScIlv2-2A-ScIlv5-2A-ScIlv3 using homologous recombination in yeast.

Plasmid pRSII416-TDH3-LlkivDmit-2A-ScADH7mit: The TDH3-LlkivDmit-2A-ScADH7mit fragment was amplified from pUG72-TDH3-LlkivDmit-2A-ScADH7mit using primers S31 and S32. The amplicon was ligated into the *Apa*I/*Sma*I site of pRSII416 to yield pRSII416-TDH3-LlkivDmit-2A-ScADH7mit.

Plasmids pRSII426Tef1-ScHXT7_F79S, pRSII426Tef1-SsXYL1, pRSII426Tef1-SsXYL2 and pRSII426Tef1-ScIlv2-2A-ScIlv5-2A-ScIlv3-Ura3: The P_{TEF1}-gene-T_{CYC1} cassette for each of the gene was amplified from its corresponding low-copy plasmid using primers S33 and S34. Each amplicon was individually ligated to the *Not*I/*Sac*I site of pRSII426 to yield the high-copy plasmid.

Plasmid pRSII426Tef1-SsXKS: The P_{TEF1}-SsXKS-T_{CYC1} cassette was amplified from pRS416Tef1-SsXKS-Ura3 using primers S35 and S36. The amplicon was ligated into the *Pst*I/*Not*I site of pRSII426 to yield pRSII426Tef1-SsXKS.

Plasmid pRSII426-TDH3-LlkivDmit-2A-ScADH7mit: The P_{TDH3}-LlkivDmit-2A-ScADH7mit-T_{CYC1} cassette was amplified from pRSII416-TDH3-LlkivDmit-2A-ScADH7mit using primers S37 and S34. The amplicon was ligated into the *Not*I/*Sac*I site of pRSII426 to yield pRSII426-TDH3-LlkivDmit-2A-ScADH7mit.

Plasmid p414-TEF1p-Cas9-CYC1t-HIS: The *TRP1* selectable marker in p414-TEF1p-Cas9-CYC1t [26] was replaced with the *HIS3* selectable marker. The *HIS3* gene fragment was amplified from the pSH62 plasmid using primers HIS3-hom-F and HIS3-hom-R. The 1.2 kb PCR band was gel purified and then mixed with the purified *Mfe*I-digested p414-TEF1p-Cas9-CYC1t fragment to form p414-TEF1p-Cas9-CYC1t-HIS via homologous recombination in *S. cerevisiae*.

Plasmid pRPR1-gRNA-CCR4: The gRNA-CCR4 fragment was amplified from the genomic DNA of PWY2353ev34 using primers CCR4_gRNA_F and univl_gRNA_R. The 0.13-kb PCR band was gel purified and ligated to the *Hin*dIII/*Xho*I site of pRPR1-gRNA handle-RPR1t [25] to yield pRPR1-gRNA-CCR4.

Plasmid pRPR1-gRNA-TIF1: The gRNA-TIF1 fragment was amplified from the genomic DNA of PWY2353ev34 using primers TIF1_gRNA_F and univl_gRNA_R. The 0.13-kb PCR band was gel purified and ligated to the *Hin*dIII/*Xho*I site of pRPR1-gRNA handle-RPR1t to yield pRPR1-gRNA-TIF1.

Plasmid pJET1.2-CCR4_A638S-donor: PCR-based Site Directed Mutagenesis was employed to generate the CCR4_A638S-donor DNA fragment that contains the point mutation in *CCR4* observed in PWY2353ev34 as well as to remove the PAM site adjacent to the crRNA target. Two overlapping fragments were amplified from the genomic DNA of PWY2353ev34 using 2 sets of primers: upstream mutation point, CCR4_seq_F and CCR4_don_R1; downstream mutation point, CCR4_don_F2 and CCR4_seq_R. To combine the upstream and downstream PCR fragments, the second PCR was performed using primers CCR4_seq_F and CCR4_seq_R. The 1-kb PCR band was gel purified and ligated with the blunt pJET1.2 cloning vector (Thermo Fisher Scientific) to yield pJET1.2-CCR4_A638S-donor.

Plasmid pJET1.2-TIF1_A79S-donor: PCR-based Site Directed Mutagenesis was employed to generate the TIF1_A79S-donor DNA fragment that contains the point mutation in *TIF1* observed in PWY2353ev34 as well as to remove the PAM site adjacent to the crRNA target. Two overlapping fragments were amplified from the genomic DNA of PWY2353ev34 using 2 sets of primers:

upstream mutation point, TIF1_seq_F and TIF1_don_R1; downstream mutation point, TIF1_don_F2 and TIF1_seq_R. To combine the upstream and downstream PCR fragments, the second PCR was performed using primers TIF1_seq_F and TIF1_seq_R. The 1-kb PCR band was gel purified and ligated with pJET1.2. The 1-kb PCR band was gel purified and ligated with the blunt pJET1.2 cloning vector (Thermo Fisher Scientific) to yield pJET1.2- TIF1_A79S-donor.

2.3 Screening of XR-XDH variants in *S. cerevisiae*

Engineered strains harboring different combination of XR-XDH variants were pre-cultured in 5-mL aliquots in SD selective yeast medium (6.7 g/L of Yeast Nitrogen Base (Difco), 20 g/L glucose, and a mixture of appropriate nucleotide bases and amino acids (CSM) overnight and used to inoculate 10 mL SX selective yeast medium (6.7 g/L of Yeast Nitrogen Base (Difco), 20 g/L xylose, and a mixture of appropriate nucleotide bases and amino acids (CSM) to achieve an initial optical density of 0.05 at 600 nm (OD_{600}). The cultures were grown at 30 °C and 250 rpm in an orbital shaking incubator. Samples were taken at 24, 48 and 72 h time points for OD_{600} measurement.

2.4 Adaptive Laboratory Evolution (ALE) of PWY2353

The parental strain (PWY2353) was cultured in 5 mL yeast minimal medium SD-URA containing 2% glucose (6.7 g/L of Yeast Nitrogen Base (Difco), 20 g/L glucose, and a mixture of appropriate nucleotide bases and amino acids with Uracil dropouts) in a 50 mL tube at 30° C and 250 rpm in an orbital shaking incubator for 16 h. The overnight cultures were transferred to fresh 20 mL SX-URA medium containing 2% D-xylose (6.7 g/L of Yeast Nitrogen Base (Difco), 20 g/L D-xylose, and a mixture of appropriate nucleotide bases and amino acids with Uracil dropouts (CSM-URA)) to obtain an initial OD_{600} of 0.01 and the cells were grown until the exponential phase was reached. Then, the cells were subcultured again into fresh 20 mL SX-URA media and this process was repeated for a total of 12 rounds. The cells from the last round were diluted and spread on SX-URA agar plates. The plates were incubated at 30° C for 3 days and 40 biggest colonies were selected and cultured in SX-URA broth. OD_{600} measurement of cells was performed to verify growth at various times till 48 h.

Specific growth rates for four selected strains were obtained using the BioLector microfermenter system (m2p labs). The strains were pre-cultured in 5 mL SD-URA medium at 30° C in an orbital shaking incubator at 250 rpm for 16 h. The overnight cultures were washed and diluted with water to obtain an OD_{600} of 2.0, and 25 uL aliquots of the diluted cultures were used to inoculate 975 uL SX-URA medium in a 48-well microflower plate. The cultures were cultivated in the BioLector microfermenter (m2p labs) at 30 ºC at 1100 rpm for 48 hours for real time measurement of biomass, pH and dissolved oxygen. The experiments were performed in biological triplicate. Scattered light measurements from the BioLector were converted to biomass (dry cell weight) by generating a standard curve using exponentially grown *S. cerevisiae* BY4742 cells and comparing a dilution series on the BioLector and dry cell weight.

2.5 Isolation and Sequencing of Genomic DNA from Evolved Strains

The genomic DNA of evolved strains PWY2353ev17, PWY2353ev34, PWY2353ev36, PWY2353ev38 and the parental strain (PWY2353) were isolated using Wizard Genomic DNA Purification Kit (Promega). Purified genomic DNA samples were submitted to Novogene for whole genome re-sequencing. Quality control of the 150 nt pair-end reads were performed using FASTP [33], and the clean sequences were then mapped against the genome sequence of *S. cerevisiae* S228C via BWA-MEM version 0.7.17 [34]. The genomic variant calling for all strains was analyzed using the Genome Analysis Toolkit (GATK4) [35]. The mutated genes *CCR4* and *TIF1* were amplified using primers CCR4_seq_F and CCR4_seq_R, TIF1_seq_F and TIF1_seq_R, respectively, for sequence confirmation. The sequencing data were deposited in Genbank as follows (strain, accession number): PWY2353, SAMN14558819; PWY2353ev17, SAMN14558820; PWY2353ev34, SAMN14558821; PWY2353ev36, SAMN14558822; PWY2353ev38, SAMN14558823.

2.6 Markerless Genome Editing of PWY2353 to Generate Point Mutations

The CRISPR/Cas9 system was employed to edit the genome of PWY2353 to generate specific point mutations [26]. Donor DNA for CCR4_A638S and TIF1_A79S were amplified from plasmids pJET1.2-CCR4_A638S-donor and pJET1.2-TIF1_A79S-donor using primers CCR4_seq_F and CCR4_seq_R, and TIF1_seq_F and TIF1_seq_R, respectively. The 1-kb PCR band of each donor DNA was gel purified and then transformed into competent PWY2353 cells along with the corresponding gRNA

plasmid and p414-TEF1p-Cas9-CYC1t-HIS. Colony PCR of transformants were performed using the corresponding primers. These are: primers CCR4_seq_F and CCR4_seq_R for PWY2353 *CCR4::CCR4*$_{A638S}$ (named PWY2383); primers TIF1_seq_F and TIF1_seq_R for PWY2353 *CCR4::CCR4*$_{A638S}$ *TIF1::TIF1*$_{A79S}$ (named PWY2393). The PCR products were gel purified and sequenced to verify the point mutation in the genome. Specific growth rates for PWY2383 and PWY2393 were obtained using the BioLector microfermenter system (m2p labs) as described in **Section 2.4**.

2.7 Integrating an additional copy of the isobutanol pathway genes into the genome of PWY2353ev34.

To integrate one additional copy each of *Ll*kivD and *Sc*ADH7 into the genome of PWY2353ev34, the *Ll*kivDmit-T2A-*Sc*ADH7mit expression construct, which also contains the URA3 marker, was amplified from plasmid pUG72-TDH3-LlkivDmit-2A-ScADH7mit[36] using primers ARS416_int_F and ARS416_int_R. These primers contain 42-bp overhangs on either side that are homologous to the *ARS416* integration site. This integration site, along with the *ARS1014* integration site used for the second round of integration, has previously been shown to lead to high expression level of the inserted gene [27]. The PCR product was gel-purified and transformed into PWY2353ev34 to create strain PWY2353ev34a. The marker gene (URA3) was removed by using the strategy described in **Section 2.1**. To verify the genetic stability of the engineered strain, PWY2353a's genomic DNA was isolated (Promega Wizard Genomic DNA Purification kit) and then subjected to a diagnostic PCR amplification that amplified regions both upstream and downstream of the integration/deletion sites.

To integrate one additional copy each of *Sc*Ilv2, *Sc*Ilv5 and *Sc*Ilv3 into the genome of PWY2353ev34a, the *Sc*Ilv2-T2A-*Sc*Ilv5-T2A-*Sc*Ilv3 expression construct, which also contains the URA3 marker, was amplified from plasmid pRS416Tef1-ScIlv2-2A-ScIlv5-2A-ScIlv3[36] using primers ARS1014_int_F and ARS1014_int_R. These primers contain 42-bp overhangs on either side that are homologous to the *ARS1014* integration site. The PCR product was gel-purified and transformed into PWY2353ev34a to create strain PWY2353ev34b. Removal of the URA3 marker gene and strain verification were performed as described above.

2.8 Quantification of Isobutanol Production in Engineered Strains

Engineered strains were pre-cultured in 5-mL aliquots in a yeast minimal medium SD-URA overnight and used to inoculate 10 mL minimal yeast medium SX-URA in 50-mL Falcon tubes to achieve an initial OD_{600} of 0.05. The cultures were grown at 30 °C and 250 rpm in an orbital shaking incubator. Samples were taken at 10, 24, 48, 72 and 144 h to determine OD_{600}, biomass, extracellular metabolites and production of higher alcohols. The amount of isobutanol and other extracellular metabolites were determined using high-performance liquid chromatography (HPLC) as previously reported with small modifications [36]. Briefly, 1 mL of culture was centrifuged at 18,000*g* for 5 min and the supernatant was filtered through 0.2 μm nylon syringe filter (Filtrex). The purified sample was then applied to an Agilent 1100 series HPLC equipped with an Aminex HPX-87H ion exchange column (Biorad). The LC program was performed using 5 mM H_2SO_4 as the solvent at a flow rate of 0.68 mL/min for 30 min. The column was maintained at 60 °C. All metabolites were detected with Agilent 1200 series DAD and RID detectors.

2.9 RNA isolation and transcript quantification

Strains were pre-cultured in 5-mL aliquots in yeast minimal medium SD-URA overnight and used to inoculate 5 mL minimal yeast medium SX-URA in 50-mL falcon tubes to achieve an initial OD_{600} of 0.05. After 48 hours, a 1 mL aliquot of each culture was collected and centrifuged for 2 min at 9000 *g*. Total RNA was extracted using the QIAgen RNeasy Kit under the manufacturer's protocol. Contaminating genomic DNA was removed from the RNA samples by DNaseI (NEB) digestion using the manufacturer's protocol. The RNA quantity was analyzed using a NanoDrop ND-1000 spectrophotometer (NanoDrop Technologies), and samples were stored at −80 °C until RT-PCR analysis. cDNA was obtained using RevertAid Reverse Transcriptase (Thermo Fisher Scientific) using the manufacturer's protocol. Relative expression levels of *LlkivD-ScADH7, ScIlv2-ScIlv5-ScIlv3 and ScATF1* were quantified using iQ SYBR Green Kit (Biorad) on CFX96 Touch Real-time PCR Detection System (Biorad). Real-time PCR was performed in triplicates, and *ScTAF10*, a gene that encodes a subunit of transcription factor IID (TFIID), was used to normalize the amount of the total mRNA in all samples. Primers for Real-time PCR are listed in **Table S1**.

3. Results and discussion

Recent works in the design and construction of robust cell factories for efficient conversion of xylose into biofuels can be grouped into three complementary strategies: 1) introduction of a xylose assimilation pathway that is stoichiometrically advantageous with regards to the biofuel of interest; 2) introduction of a xylose-specific transporter; and 3) introduction of specific gene knockouts to improve xylose utilization [11, 13]. We designed our isobutanol producing strain by combining these strategies. For the first strategy, we used the conventional xylose reductase-xylose dehydrogenase pathway as it has a higher pyruvate yield based on stoichiometry when compared with the xylulose-1-phosphate (X-1-P) pathway (1.67 vs. 1 mol/mol xylose) [37]. The synthetic X-1-P pathway, which converts xylose into xylulose-1-phosphate, before an aldolytic cleavage produces glycoaldehyde and dihydroxyacetone phosphate (DHAP), is more advantageous for the production of C2 chemicals such as ethylene glycol [38]. The xylose isomerase (XI) pathway, while having a similar pyruvate yield as the XR-XDH pathway, suffers from low catalytic efficiency of the isomerase enzyme as well as the difficulty of functionally expressing bacterial XI enzymes in *S. cerevisiae* [39–41]. For the second strategy, we introduced a re-engineered hexose transporter HXT7 into *S. cerevisiae* [42]. Apel and coworkers discovered a F79S point mutation in HXT7 that enables the hexose transporter to transport xylose into the cell with high efficiency. For the last strategy, we disrupted the aldose reductase gene *GRE3* and the alkaline phosphatase *PHO13* as previous reports indicated that deletion of these genes improved xylose utilization [43, 44].

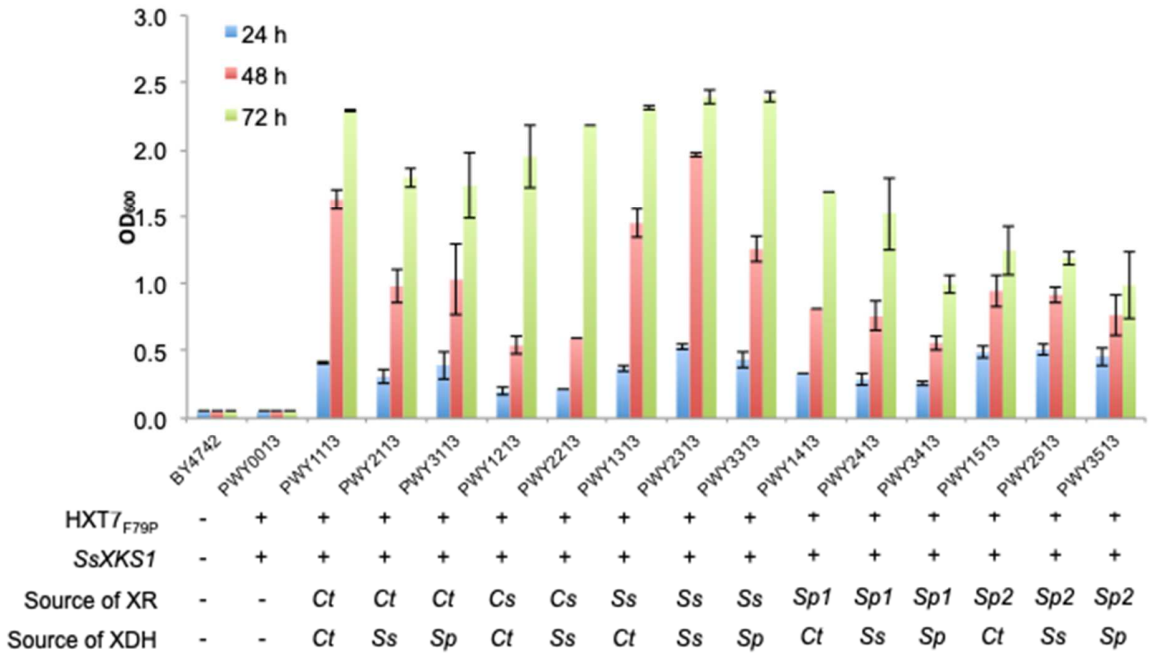

Figure 2. Growth profile of engineered *S. cerevisiae* harboring different XR-XDH variants in *S. cerevisiae*. Engineered strains were pre-cultured in 5-mL aliquots in yeast minimal medium (2% glucose) overnight and used to inoculate 10 mL yeast minimum medium (2% xylose) to achieve an initial optical density of 0.05 at 600 nm (OD_{600}). The cultures were grown at 30 °C and 250 rpm in an orbital shaking incubator. Samples were taken at 24, 48 and 72 h time points for OD_{600} measurement. Values are the mean of three biological replicates ± standard deviation (n = 3). *Ct*, *Candida tropicalis*; *Cs*, *Candida shehatae*; *Ss*, *Scheffersomyces stipitis*; *Sp*, *Spathaspora passalidarum*; *Sp1*, *Spathaspora passalidarum XYL1.1*; *Sp2*, *Spathaspora passalidarum XYL1.2*

3.1 Screening of optimal xylose reductase-xylose dehydrogenase pathway genes

To engineer *S. cerevisiae* with the ability to grow on xylose, we first integrated the xylose-specific variant of the sugar transporter *HXT7* (*$HXT7_{F79S}$*) and a copy of the *S. stipitis* xylulokinase gene (*XYL3*) into BY4742, a laboratory strain of *S. cerevisiae*. While a gene encoding xylulokinase is present in *S. cerevisiae* (i.e. *XKS1*), its expression level is insufficient for efficient conversion of xylulose to xylulose-5-phosphate [45]. The resulting strain, PWY0013, while still unable to grow in minimal medium containing xylose as the sole carbon source, provided the necessary background for XR-XDH screening (**Figure 1**). We screened different XR and XDH candidate enzymes that have demonstrated high activity in *S. cerevisiae* [46–48]. For XR, these are *Ct*XYL1

from *Candida tropicalis*, *Cs*XR from *Candida shehatae*, *Ss*XYL1 from *Scheffersomyces stipitis*, *Sp*XYL1.1 from *Spathaspora passalidarum* and *Sp*XYL1.2 from *Spathaspora passalidarum*. The first four enzymes perfer NADPH as the redox cofactor while the last enzyme prefers NADH. For XDH, these are *Ct*XDH from *Candida tropicalis*, *Ss*XYL2 from *Scheffersomyces stipitis*, and *Sp*XYL2 from *Spathaspora passalidarum*. To ensure robust and stable expression of these genes, we integrated the individual XR and XDH constructs into the *ARS308* and *ARS720* sites, respectively. These chromosomal integration sites have previously been shown to lead to high expression level of the inserted gene [27].

The engineered strains exhibited superior cell growth when compared to strains BY4742 (lab strain [49]) and PWY0013 (**Figure 2, Table 3**). Overall, the choice of XR appeared to affect cell growth more so than the choice of XDH. In particular, strains expressing XR from *S. stipitis* performed the best, reaching the final OD_{600} (after 72 h) of 2.32 - 2.40, while strains harboring either XR variants from *S. passalidarum* performed the worst, reaching the final OD_{600} of 0.99 -1.69. Interestingly, strains harboring XR from *C. shehatae* grew slowly within the first 48 hours, reaching an OD_{600} of ~ 0.5, but then grew rapidly in the final 24 hours to reach an OD_{600} of 2.0 – 2.2. Despite several attempts, we were unable to obtain a viable strain overexpressing XR from *C. shehatae* and XDH from *S. passalidarum*. Strains PWY2313, which harbors XR and XDH from *S. stipitis*, and PWY1113, which harbors XR and XDH from *C. tropicalis*, achieved the highest OD_{600} after 48 h at 1.96 and 1.63, respectively, and were used in subsequent engineering steps.

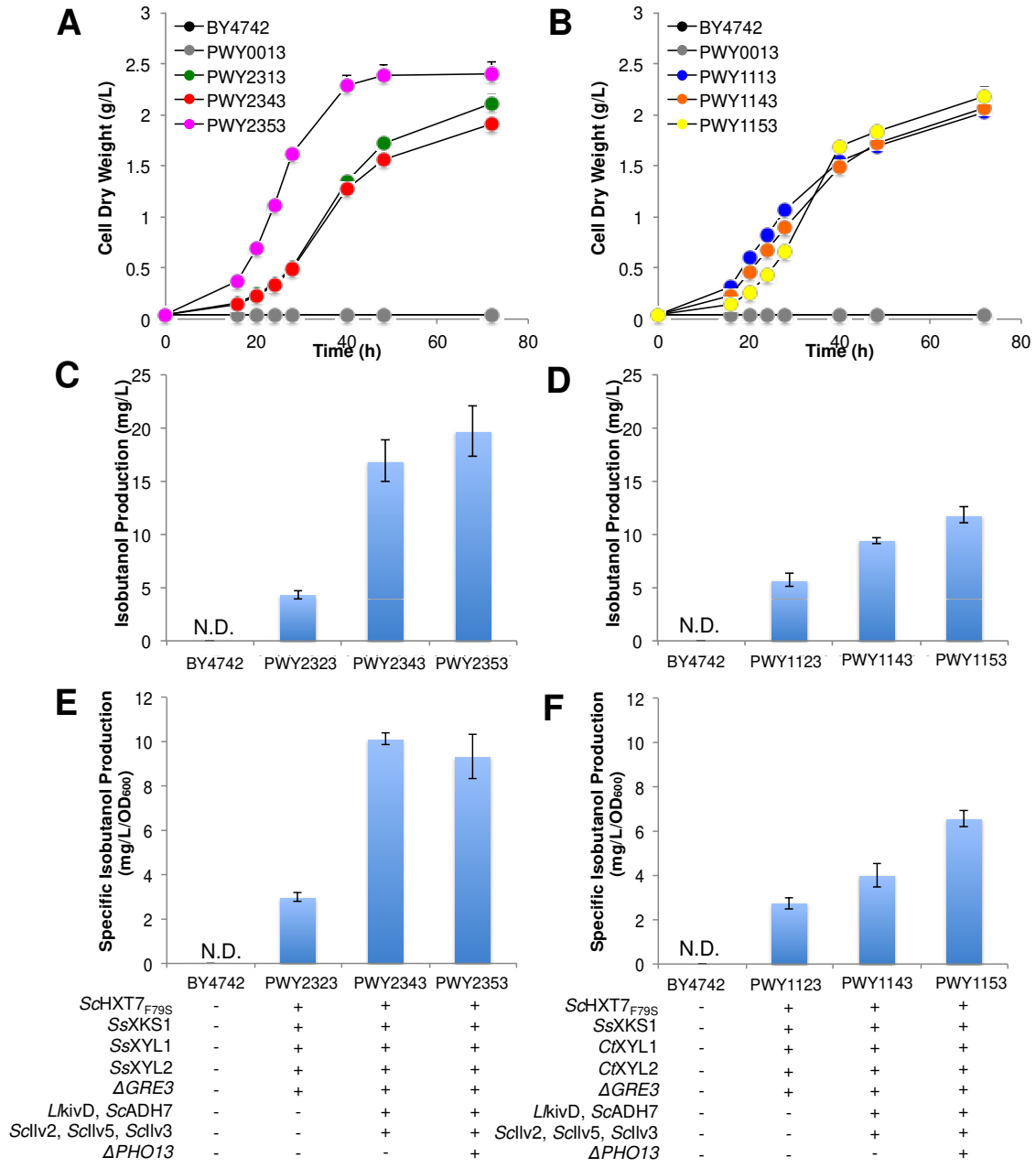

Figure 3. Growth profile and isobutanol production of engineered strains in minimal medium containing 2% xylose. Growth profiles of engineered strains expressing XR-XDH from *S. stipitis* (A) and *C. tropicalis* (B). Total (C) and specific (E) isobutanol production after 2 days of engineered strains expressing XR-XDH from *S. stipitis*. Total (D) and specific (F) isobutanol production after 2 days of engineered strains expressing XR-XDH from *C. tropicalis*. Engineered strains were pre-cultured in 5-mL aliquots in SD minimal medium overnight and used to inoculate 10 mL fresh SX (2% xylose) to achieve an initial optical density of 0.05 at 600 nm (OD_{600}). The cultures were grown at 30 °C and 250 rpm in an orbital shaking incubator. Samples were taken after 2 days and the

supernatants were analyzed on HPLC to quantify the isobutanol content. Values are the mean of three biological replicates ± standard deviation (n = 3). N.D. represents not detected due to strain's inability to grow. *Sc*, *Saccharomyces cerevisiae*; *Ss*, *Scheffersomyces stipitis*; *Ct*, *Candida tropicalis*.

3.2 Integration of isobutanol pathway genes for production of isobutanol from xylose

To engineer isobutanol production in the yeast *S. cerevisiae*, we integrated the non-fermentative isobutanol pathway that combines the L-valine biosynthetic and ketoacid degradation pathways (**Figure 1**) [5]. This synthetic isobutanol pathway, pioneered by Atsumi and coworkers, involves "hijacking" the native amino acid metabolism of the host organism and diverts the amino acid intermediate to the 2-keto acid degradation pathway for higher alcohol production. In the L-valine biosynthetic pathway, acetolactate synthase (Ilv2) condenses two molecules of pyruvate to 2-acetolactate, which is then reduced to 2,3-dihydroxyisovalerate by acetohydroxyacid reductoisomerase (Ilv5). Next, 2,3-dihydroxyisovalerate is converted to 2-ketoisovalerate, a key intermediate in L-valine biosynthesis, by dihydroxyacid dehydratase (Ilv3). In the ketoacid degradation pathway, 2-ketoisovalerate is converted to isobutanal by introducing a heterologous ketoacid decarboxylase (kivD) from the bacterium *Lactococcus lactis* or by overexpression of the endogenous decarboxylase (Aro10). The resulting aldehyde is then reduced by an alcohol dehydrogenase (Adh7 or Adh2) from *S. cerevisiae* to the final alcohol products, including isobutanol.

While production of isobutanol from glucose in the yeast system is well established, production from xylose has been much less studied, with only one published work from Brat and Bowles [21]. In their system, the xylose isomerase XylA from *Clostridium phytofermentans* was heterologously expressed in *S. cerevisiae*, along with overexpression of the endogenous transaldolase TAL1 and xylulokinase XKS1. For the isobutanol pathway, the authors opted to relocalize the L-valine pathway enzymes Ilv2, Ilv5 and Ilv3 from the mitochondria to cytosol as well as overexpress the endogenous decarboxylase Aro10 and alcohol dehydrogenase Adh2. The resulting strain produced 1.36 mg/L isobutanol from 20 g/L xylose, which corresponds to an isobutanol yield of 0.16 mg/g xylose.

In deciding the localization of the isobutanol pathway enzymes, we contend that targeting the five enzymes to the mitochondria is a more appropriate strategy. Growth on xylose and other non-fermentable sugars has been shown to dis-regulate glucose-dependent repression of mitochondria development and induce its metabolism [50, 51]. For the choice of the keto-acid degradation pathway enzymes, we chose the keto-acid decarboxylase LlkivD from *L. lactis* and the endogenous alcohol dehydrogenase ADH7 based on a previous report by Avalos and co-workers that demonstrated robust activities of the two enzymes when they were both targeted to the mitochondria [52]. To incorpotate the isobutanol pathway into PWY1113 and PWY2313, we linked genes from each pathway together with the self-cleaving 2A peptide sequence from the foot-and-mouth disease virus (FMDV) [53] and separately placed them behind the strong constitutive promoters P_{TEF1} and P_{TDH3}. This ensures stoichiometric production of all the proteins whose genes are linked together by the 2A peptide sequence. The mitochondrial signal peptide sequence was added to *LlkivD* and *ADH7* to target the enzymes to the mitochondria. Finally, to increase xylose utilization, we deleted the endogenous aldose reductase gene *GRE3* as well as the alkaline phosphatase gene *PHO13*. These deletions have been used to improve xylose utilization in *S. cerevisiae* expressing either the XR-XDH or XI pathway [54].

Gratifyingly, we observed isobutanol production in our engineered strains (**Figure 3, Table 3**). Overall, strains overexpressing XR and XDH from *S. stipitis* performed better, resulting in greater cell growth and higher isobutanol levels. In particular, strain PWY2343, which expresses XR and XDH from *S. stipitis* as well as the complete isobutanol pathway, produced 16.9 ± 1.9 mg/L of isobutanol (specific isobutanol production of 10.1 ± 0.3 mg/L/OD_{600}; specific growth in xylose of 0.0431 $\pm$0.0004 h^{-1}) after 2 days of cultivation. The deletion of *PHO13* in strain PWY2343 to create strain PWY2353 further improved isobutanol titer to 19.7 ± 2.4 mg/L (specific isobutanol production of 9.3 ± 1.0 mg/L/OD_{600}; specific growth in xylose of 0.0532 $\pm$0.0004 h^{-1}). In comparison, the most effective strain expressing XR and XDH from *C. tropicalis* (strain PWY1353) produced isobutanol at a titer of only 11.8 $\pm$0.8 mg/L (specific isobutanol production of 6.6 ± 0.4 mg/L/OD_{600}; specific growth in xylose of 0.0513 $\pm$0.0002 h^{-1}).

3.3 Improving isobutanol titer by fine-tuning the expression levels of the biosynthetic pathway genes

To further improve the isobutanol production titer in PWY2353, we turned our attention to fine-tuning the expression levels of the biosynthetic pathway genes. A large body of work in metabolic engineering indicates that the expression levels of metabolic pathway genes greatly impact the production levels of the compound of interest [3]. Too low expression levels lead to bottlenecks while too high expression levels can deplete the cellular resources that could otherwise be used to produce the compound of interest. To this end, we studied the effect of additional copies of the XR-XDH pathway genes, the isobutanol pathway genes, as well as the transporter and xylulokinase genes. We used the CEN6/ARS4 and 2μm plasmid-expression for low and high-copy expression, respectively [23]. The yeast CEN6/ARS4 origin of replication resulted in transformants with a low copy plasmid number (1 copy per cell). In contrast, the yeast 2**μ** origin of replication allowed autonomous replication of the plasmids and resulted in transformants with a high plasmid copy number (10–40 copies per cell). We also extended fermentation time to 6 days to increase isobutanol titer as well as to allow a more direct comparison to the previous report by Brat and Boles [21].

We obtained mixed success with high-copy plasmid-based overexpression (**Figure 4**). Notably, high-copy plasmid-based expression of *Ll*kivD and *Sc*ADH7 led to the highest total isobutanol production at 47.7 ± 5.0 mg/L, a 45% increase from the control strain (PWY2353 harboring an empty high-copy vector) at 32.9 ± 1.7 mg/L after 6 days of cultivation. This improved strain (PWY2343 harboring pRSII426-*Ll*kivD-*Sc*ADH7) consumed more xylose and produced lower levels of the side products glycerol and xylitol. In contrast, additional copies of either $HXT7_{F79S}$ or SsXDH resulted in less xylose consumption as well as decreases in total isobutanol production (21.9 ± 1.5 mg/L and 25.5 ± 4.6 mg/L, respectively).

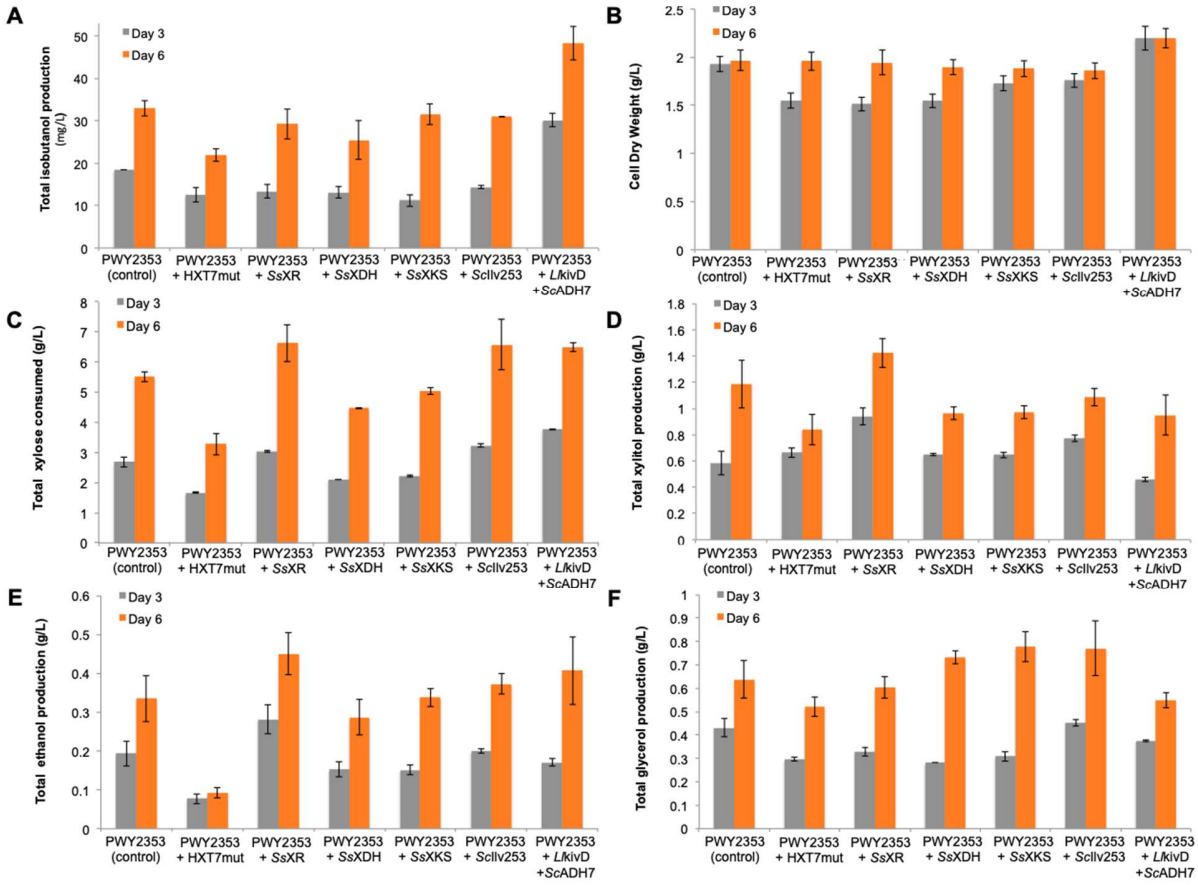

Figure 4. Characterization of engineered strains with high-copy (2μm) plasmid-based overexpression of individual pathway genes. Total isobutanol production (A), cell dry weight (B), xylose consumption (C), xylitol production (D), ethanol production (E), and glycerol production (F). Individual gene construct was placed in the pRSII426 plasmid and transform into PWY2353. The resulting strains were cultured in minimal medium containing 2% xylose as the sole carbon source. Values are the mean of three biological replicates ± standard deviation (n = 3) after 3 and 6 days.

We observed similar results with low-copy plasmid-based expression (**Figure 5**). Specifically, overexpression of *Ll*kivD and *Sc*ADH7 improved isobutanol titer to 48.4 ± 2.0 mg/L (specific isobutanol production of 21.5 ± 2.0 mg/L/OD_{600} ; yield of 7.0 mg/g consumed D-xylose), which is 40% higher than in the control strain (PWY2343 harboring an empty vector) and approximately 36 folds higher than that from the previous report by Brat and Boles (total isobutanol production of 1.36 ± 0.11 mg/L after 146 h of cultivation). The increase in isobutanol of this strain (PWY2343

harboring pRSII416-*Ll*kivD-*Sc*ADH7) was accompanied by a decrease in the formation of the side products ethanol and glycerol (**Figure 5**), while biomass, xylose consumption and xylitol formation remained unchanged. Accumulatively, our results from both high-copy and low-copy plasmid-based overexpression indicate that overexpression of the terminal enzymes (i.e. those leading directly to the final product isobutanol) had the largest effect on isobutanol titers.

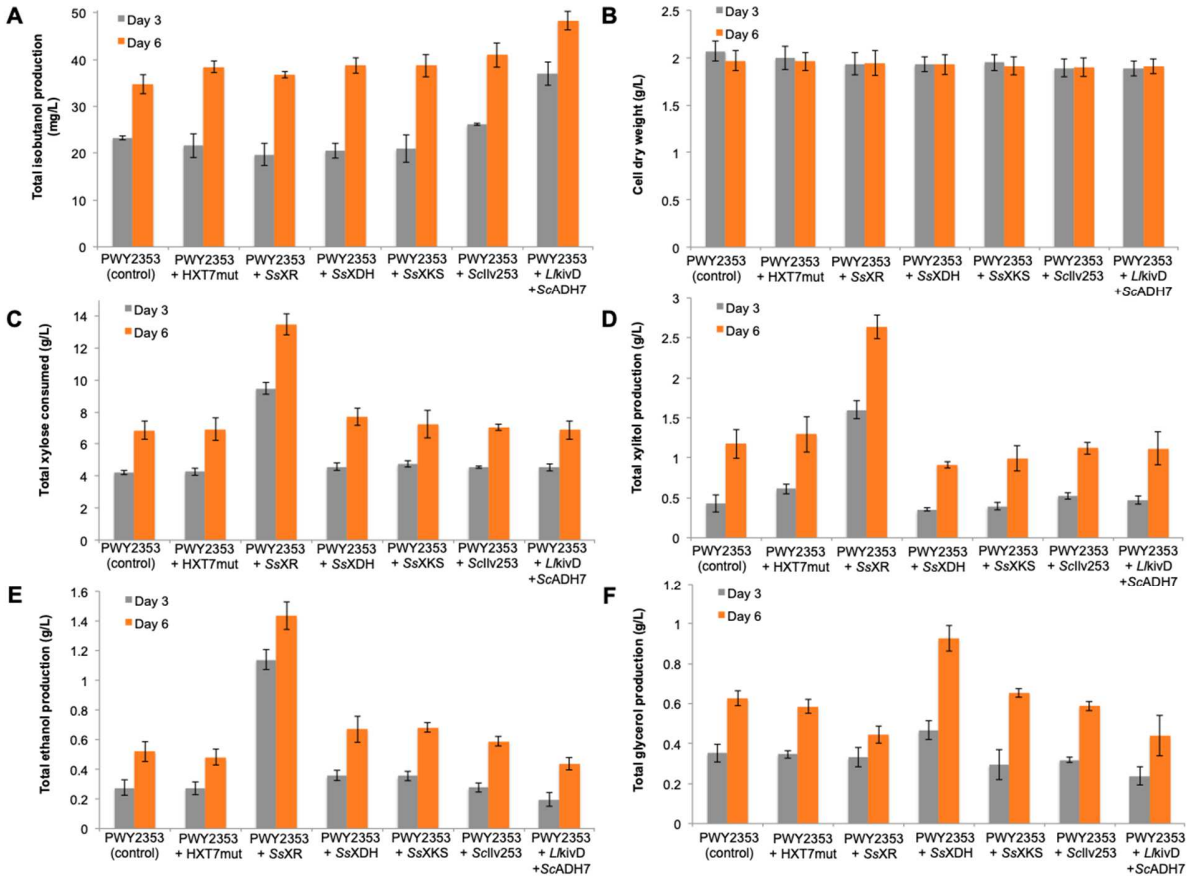

Figure 5. Characterization of engineered strains with low-copy plasmid-based overexpression of individual pathway genes. Total isobutanol production (A), cell dry weight (B), xylose consumption (C), xylitol production (D), ethanol production (E), and glycerol production (F). Individual gene construct was placed in the pRSII416 plasmid and transform into PWY2353. All strains were cultured in minimal medium containing 2% xylose as the sole carbon source. Values are the mean of three biological replicates ± standard deviation (n = 3) after 3 and 6 days.

Table 4. Production of isobutanol and other metabolites in engineered and evolved strains

Strain name	Isobutanol titer in xylose (mgL^{-1})	Specific Isobutanol Production (mg $gDCW^{-1}$)	Isobutanol productivity after 2 days (6 days) in xylose (mg $gDCW^{-1}h^{-1}$)	Ethanol titer (g/L)	Xylitol titer (g/L)
PWY2353	48.9 ± 2.8	23.9 ± 1.4	0.291 ± 0.037 (0.166 ± 0.010)	0.569 ± 0.022	0.928 ± 0.175
PWY2353ev17	36.0 ± 2.5	20.1 ± 1.5	0.206 ± 0.009 (0.140 ± 0.010)	0.190 ± 0.006	0.412 ± 0.024
PWY2353ev34	60.6 ± 1.3	31.6 ± 1.8	0.392 ± 0.032 (0.220 ± 0.013)	0.254 ± 0.002	1.014 ± 0.014
PWY2353ev36	49.2 ± 3.6	24.9 ± 1.9	0.307 ± 0.015 (0.173 ± 0.013)	0.598 ± 0.027	1.224 ± 0.091
PWY2353ev38	25.6 ± 2.3	12.0 ± 1.1	0.148 ± 0.015 (0.083 ± 0.007)	0.321 ± 0.004	1.037 ± 0.027
PWY2363	63.8 ± 8.4	30.7 ± 0.8	0.441 ± 0.027 (0.213 ± 0.005)	0.546 ± 0.007	1.218 ± 0.052
PWY2373	66.7 ± 2.1	32.4 ± 1.2	0.385 ± 0.022 (0.225 ± 0.008)	0.683 ± 0.010	1.089 ± 0.036
PWY2353ev34a	74.1 ± 3.0	39.6 ± 2.3	0.487 ± 0.008 (0.275 ± 0.016)	0.289 ± 0.014	0.999 ± 0.062
PWY2353ev34b	92.9 ± 4.4	50.2 ± 2.6	0.588 ± 0.040 (0.348 ± 0.018)	0.318 ± 0.009	0.880 ± 0.017

Another engineered strain of note is PWY2353 overexpressing *Ss*XR (PWY2353 harboring pRSII416-*Ss*XR), which had the highest xylose consumption at 13.0 ± 0.5 g/L xylose, roughly twice the amount consumed in the control strain (at 6.8 ± 0.6 g/L). However, this increase in xylose consumption did not improve isobutanol production, but rather led to increases in the formation

of the pathway intermediate xylitol (2.6 ± 0.2 g/L up from 1.2 ± 0.2 g/L) and the side product ethanol (1.4 ± 0.1 g/L up from 0.5 ± 0.1 g/L). XR catalyzes the reduction of xylose to xylitol and accumulation of xylitol indicates that the next enzyme in the pathway, xylitol dehydrogenase (XDH) may be limited. Accumulation of ethanol indicates that the reduction of xylose to xylitol by XR potentially caused redox cofactor imbalances. Therefore, further strain improvement may be achieved by overexpression of an engineered XDH that has a cofactor preference for $NADP^+$ [55, 56]. Alternatively, down-regulation of the ethanol pathway by deleting the pyruvate decarboxylase gene PDC1 and the alcohol dehydrogenase genes ADH1-5 may further improve the isobutanol titer [57].

3.4 Adaptive Laboratory Evolution (ALE) of PWY2353 Led to a Strain with Improved D-Xylose Utilization

Adaptive laboratory evolution (ALE) is a powerful and widely used technique for untargeted strain improvement and has been employed in a variety of microbial hosts [58]. Notable examples of ALE in *S. cerevisiae* include the identification of genetic targets that lead to tolerance against a variety of industrially relevant stresses such as high temperature [59], high glucose concentration [60], and high medium-chain alcohols content [61]. However, ALE has not been applied to improve isobutanol production from D-xylose before. We subjected PWY2353 to an ALE experiment in the growth medium containing 2% D-xylose as the sole carbon source to enrich for *S. cerevisiae* strains with improved D-xylose utilization. The culture was grown until the exponential phase and then the cells were subcultured again into fresh medium. After repeating this process for a total of 12 rounds, we isolated 40 strains from this population as single colonies on plates and assessed their preliminary growth profile in yeast minimal medium containing 2% D-xylose as the sole carbon source (**Figure 6A**). From these, we picked the top four strains, PWY2353ev17, PWY2353ev34, PWY2353ev36 and PWY2353ev38, based on their final OD_{600} values after 48 hours, and performed a detailed study of their growth profile compared to parental (non-evolved) strain PWY2353 using the BioLector Pro microfermentor (m2p-labs) (**Figure 6B)**. Overall, the four evolved strains exhibited 26.6 - 58.3% higher specific growth rates compared to the value for PWY2353 (0.0229 ± 0.0005 h^{-1}) (**Table 4** and **Figure 6C**). In particular, strain PWY2353ev34 had

the highest specific growth rate at 0.0363 ± 0.0003 h^{-1}, followed by strain PWY2353ev36 at 0.0341 ± 0.0013 h^{-1}.

In addition to cell growth, we also looked at isobutanol production of the selected evolved strains. Interestingly, there appears to be no direct correlation between isobutanol titers and specific growth rates in the selected evolved strains. Only one evolved strain, PWY2353ev34, produced isobutanol at a higher titer (60.6 ± 1.3 mg/L) than the level observed in the non-evolved strain PWY2353 (48.9 ± 2.8 mg/L) (**Table 4**). This increase in isobutanol was accompanied by a decrease in ethanol production with strain PWY2353ev34 producing 0.254 ± 0.002 g/L, a 55% decrease from the PWY2353's value of 0.569 ± 0.022 g/L. The levels of xylitol, the only other major metabolite detected, were similar in both strains. Strain PWY2353ev36 produced isobutanol at similar titer to the PWY2353 at 49.2 ± 3.6 mg/L, while PWY2353ev17 and PWY2353ev38 produced isobutanol at lower titers of 36.0 ± 2.5 mg/L and 25.6 ± 2.3 mg/L, respectively.

Cumulatively, our results indicate that D-xylose utilization is a phenotype that can be improved by adaptive laboratory evolution and underscore the robustness of the strategy in improving desirable, industrially useful phenotypes in microbial hosts in a relatively short amount of time. Conversely, there remain many traits—for example, production of isobutanol, a compound that serves our interest but provides no apparent benefit to survival of the cell—that cannot be improved by adaptive laboratory evolution in a straightforward manner. For these traits, linking them to cell survival is critical to the success of the evolution strategy [58].

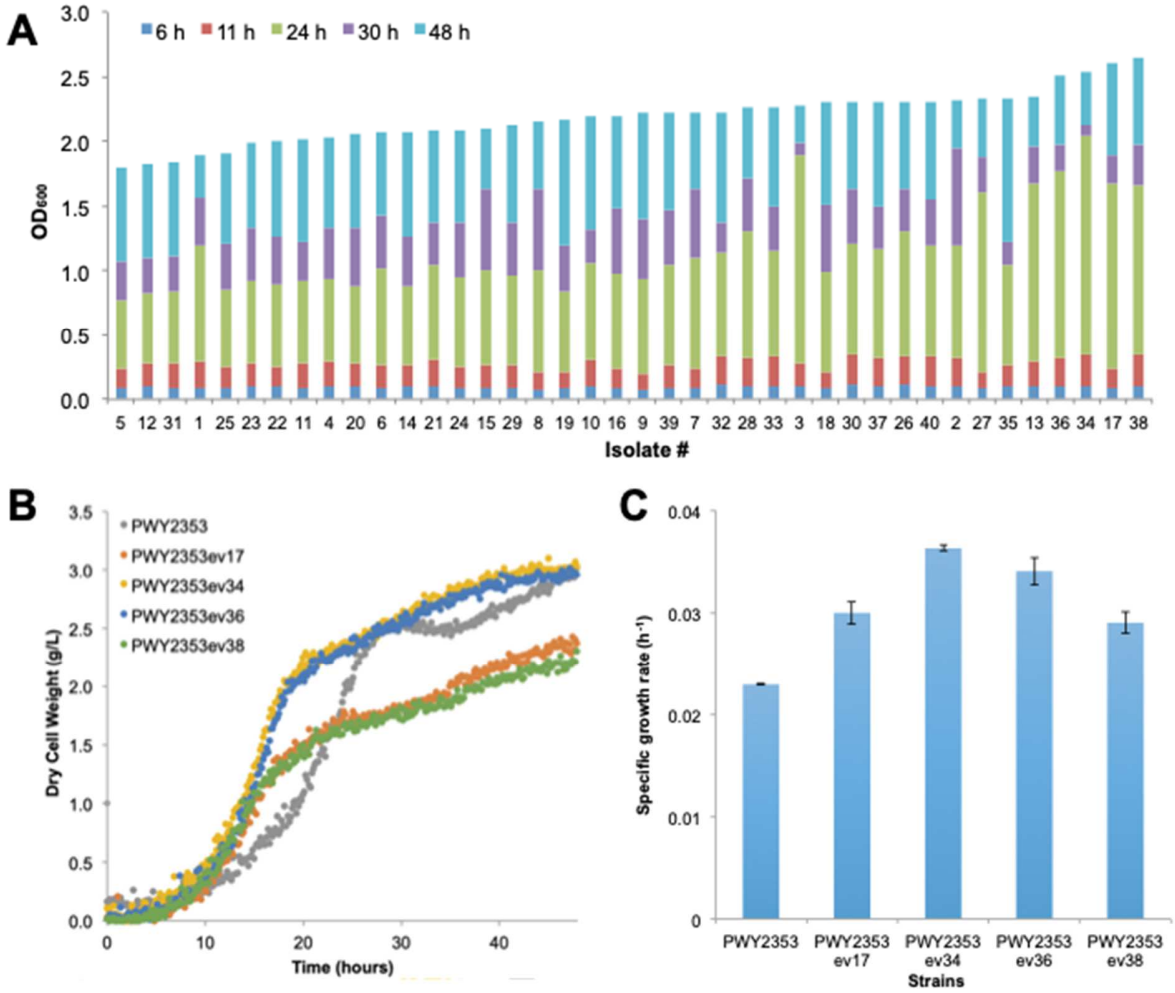

Figure 6. Adaptive laboratory evolution of PWY2353 resulted in strains with improved specific growth rates. Growth profile of 40 selected strains after 12 rounds of sub-culturing in liquid minimal medium with 2% D-xylose as the sole carbon source (**A**). Detailed growth profiles (**B**) and specific growth rates (**C**) of the four fastest-growing evolved strains and control strain (unevolved PWY2353) in yeast minimal medium with 2% D-xylose as the sole carbon source. Specific growth rates were determined using the BioLector Pro microfermentor (m2p-labs).

Table 5. Summary of mutations in evolved strains identified by whole-genome resequencing

Strain	Mutation	Gene	Protein function
PWY2353ev17	A638S	*CCR4*	3'-5'-exoribonuclease subunit of the core CCR4-NOT complex
PWY2353ev34	A638S	*CCR4*	3'-5'-exoribonuclease subunit of the core CCR4-NOT complex
	A79S	*TIF1*	a subunit of the translation initiation factor 4F complex
PWY2353ev36	A638S	*CCR4*	3'-5'-exoribonuclease subunit of the core CCR4-NOT complex
	-577T>C (nucleotide change in the promoter region)	*HXT15*	Hexose transporter
PWY2353ev38	A638S	*CCR4*	3'-5'-exoribonuclease subunit of the core CCR4-NOT complex
	S155L	*GIP2*	a regulatory subunit of phosphatase Glc7p protein

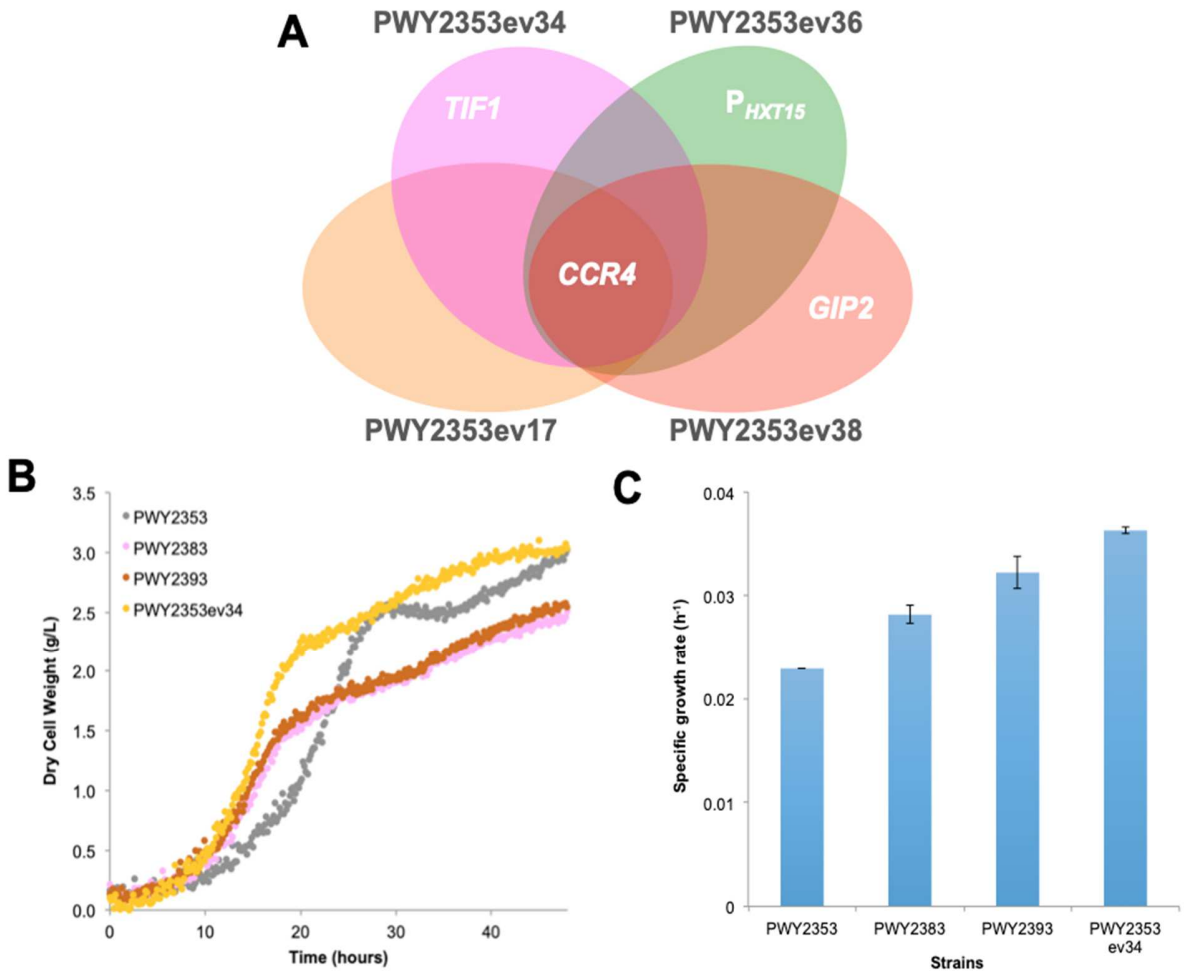

Figure 7. Genome re-sequencing of evolved strains revealed several SNPs that enable the engineered *S. cerevisiae* to more efficiently utilize D-xylose. Distribution of four genes with single nucleotide variants (SNVs) found in the four selected evolved strains (A). Detailed growth profiles (**B**) and specific growth rates (**C**) of strains PWY2383 and PWY2393, which harbor SNVs found in the evolved strain PWY2353ev34. Growth was determined using the BioLector Pro microfermentor (m2p-labs) in liquid minimal medium with 2% D-xylose as the sole carbon source.

3.5 Genome Sequencing of Evolved Strains Identified Several Key Mutations

In order to identify the specific genetic targets that lead to improved D-xylose utilization, we sequenced the genomic DNA from the top four evolved strains. We identified mutations by comparing the genome sequence of each strain with that of the parental strain (PWY2353), which

was also sequenced. All of the mutations for each strain are listed in **Table 5** and shown in **Figure 7A.** Interestingly, all four evolved strains had an A638S mutation in Carbon Catabolite Repression 4 gene (*CCR4*), which encodes the 3'-5'-exoribonuclease subunit of the core CCR4-NOT complex. Present in all eukaryotes, the CCR4-NOT complex is a multisubunit complex that performs crucial roles in several cellular pathways [62]. First, it regulates transcription at multiple steps from production and processing of messenger RNAs (mRNAs) in the nucleus to their degradation in the cytoplasm via deadenylation-dependent mRNA decay [63]. Second, the CCR4-NOT complex is involved in DNA replication and regulation of cell cycle [64]. Third, the CCR4-NOT complex controls the activity of the environmental stress transcription factor MSN2 [65]. Taken together, these previous studies demonstrate the CCR4-NOT complex's role in helping the cells respond to changes in environmental conditions. Though we were unable to find any report that implicates CCR4 in D-xylose utilization, several works indicate that the protein is required for expression of many essential genes under glucose-depletion conditions [66, 67].

Another mutation of note was the A79S mutation in the translation initiation factor eIF-4A gene (*TIF1*), an essential gene that encodes a subunit of the translation initiation factor 4F complex [68]. Translation initiation factor eIF4A is an ATP-dependent D-E-A-D box RNA helicase that accelerates the recruitment of mRNA during the assembly of 48S preinitiation complex [69]. The role of the alanine residue at position 79 of eIF-4A has previously been characterized [70]. Located directly adjacent to the ATPase A motif, A79 was proposed to affect ATP binding and ATPase activity of the enzyme. Importantly, while the yeast eIF-4A protein contains alanine at this position, the mouse variant contains a serine residue, providing evidence that the eIF-4A_A79S mutation found in PWY2353ev34 would not hamper the activity of the enzyme.

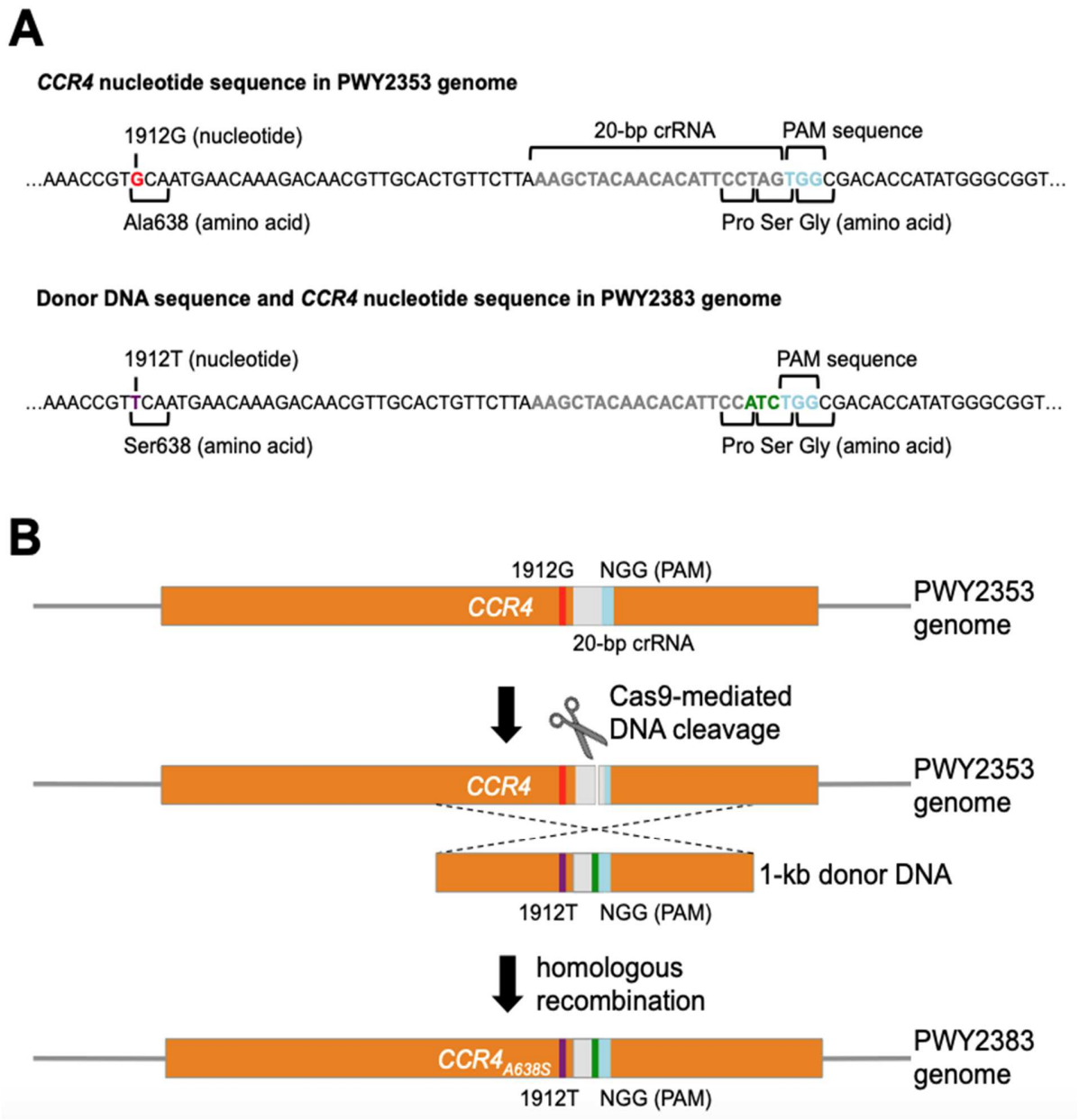

Figure 8. Strategy to reverse engineer PWY2353 with *CCR4*$_{A638S}$ to generate PWY2383

3.6 Reverse engineering of PWY2353 with *CCR4*$_{A638S}$ and *TIF1*$_{A79S}$ mutations improves D-xylose utilization

Given that PWY2353ev34 had the highest xylose specific growth rate among the evolved strains, we decided to investigate whether the mutations found in PWY2353ev34 contributed to the improved D-xylose utilization phenotype. Specifically, we reversed engineered the parental strain PWY2353 to harbor the *CCR4*$_{A638S}$ and *TIF1*$_{A79S}$ mutations. First, we employed the markerless CRISPR-Cas9 system to edit the genome of PWY2353 to harbor *CCR4*$_{A638S}$ [25, 26]. The strategy enabled us to edit a single base pair (1912G>T) in the yeast genome without the use of a selectable marker and without leaving any "scar" in the genome (**Figure 8**). The resulting strain, PWY2383, had a D-xylose specific growth rate of 0.0282 ± 0.0009 h^{-1}, which is 23.0% higher than PWY2353's value of 0.0229 ± 0.0005 h^{-1} (**Figure 7**). The A638S mutation occurs in the nuclease domain of CCR4. The crystal structure of the yeast CCR4-NOT complex has recently been solved but the alanine residue at position 638 was disordered [71]. Bioinformatics analysis of the *CCR4*$_{A638S}$ amino acid sequence using several open-source phosphorylation site prediction softwares such as NetPhos and Scansite suggested that the serine residue at 638 can serve as a phosphorylation site [72, 73]. However, when we mutated the alanine residue at position at 638 with threonine, another phosphorylatable residue, the resulting strain had a petite phenotype (**Figure S2**). Having verified the role *CCR4*$_{A638S}$ played in improving xylose growth, we next integrated *TIF1*$_{A79S}$ into the genome of PWY2383 to create strain PWY2393 (**Figure S1**). This further improved D-xylose specific growth rate to 0.0323 ± 0.0016 h^{-1}, an additional 14.4% improvement over PWY2383's value and a total of 40.6% improvement over the PWY2353's value.

3.7 Further Strain Improvement by Fine-tuning Expression of Bottleneck Enzymes

Because adaptive laboratory evolution only improved the yeast's specific growth on xylose, we turned to rational metabolic engineering to improve the isobutanol production titer. For this effort, we chose the evolved strain PWY2353ev34 due to its highest specific growth on xylose as well as its isobutanol titer. To improve the isobutanol production titer in the evolved strain PWY2353ev34, we fine-tuned the expression levels of the biosynthetic pathway genes. A

substantial amount of research in metabolic engineering suggests that the expression levels of metabolic pathway genes can impact the production levels of the compound of interest [3]. Too low an expression level leads to bottlenecks in the pathway, while too high an expression level will deplete the cellular resources that would otherwise be used to generate the target compound.

In our previous work, we varied the pathway enzyme expression levels by adding additional gene copies via the use of CEN6/ARS4 (low-copy) and 2μ (high-copy) plasmid expression systems [36]. We observed the biggest improvement in isobutanol production (a 40% increase in isobutanol titer over the parental strain) when the final two enzymes (*Ll*kivD and *Sc*ADH7) were overexpressed using the CEN6/ARS4 plasmid. The second best improvement (an 18% increase in isobutanol titer) was observed when we overexpressed the endogenous L-valine biosynthetic pathway genes (*Sc*Ilv2, *Sc*Ilv5 and *Sc*Ilv3)—also using the CEN6/ARS4 plasmid. Building upon these observations, we integrated one additional copy each of *Ll*kivD and *Sc*ADH7 into the genome of PWY2353ev34. The genes were linked together with the self-cleaving 2A peptide sequence from the foot-and-mouth disease virus (FMDV)[53] and placed behind the strong constitutive promoter P_{TDH3}. The resulting strain, PWY2353ev34a, produced isobutanol at a titer of 74.1 ± 3.0 mg/L (specific isobutanol production of 39.6 ± 2.3 mg/g DCW), which corresponds to a 22% improvement in titer over the evolved strain (**Figure 9B** and **9D, Table 4**). Encouraged by these results, we next integrated one additional copy each of *Sc*Ilv2, *Sc*Ilv5 and *Sc*Ilv3 into the genome of PWY2353ev34a. The three genes were again linked together with the self-cleaving 2A peptide sequence from FMDV, and placed behind another strong constitutive promoter P_{TEF1}. The resulting strain, PWY2353ev34b, was able to produce isobutanol at a titer of 92.9 ± 4.4 mg/L (specific isobutanol production of 50.2 ± 2.6 mg/g DCW), which corresponds to a further 25% titer improvement over strain PWY2353ev34a and a 52% improvement in titer over the evolved strain PWY2353ev34 (**Figure 9B, 9D** and **9F**). Moreover, this is a 90% improvement in titer and a 110% improvement in specific production over the non-evolved strain. As a comparison, we also integrated the *Ll*kivD-T2A-*Sc*ADH7 gene construct, either alone or in a combination with the *Sc*Ilv2-T2A-*Sc*Ilv5-T2A-*Sc*Ilv3 gene construct, into the genome of the non-evolved strain (PWY2353) to create strains PWY2363 and PWY2373, respectively. The isobutanol titers in these strains were

63.8 ± 8.4 mg/L and 66.7 ± 2.4 mg/L, while their specific isobutanol production were 30.7 ± 0.8 mg/g DCW and 32.4 ± 1.2 mg/g DCW, respectively (**Figure 9A**, **9C** and **9E**).

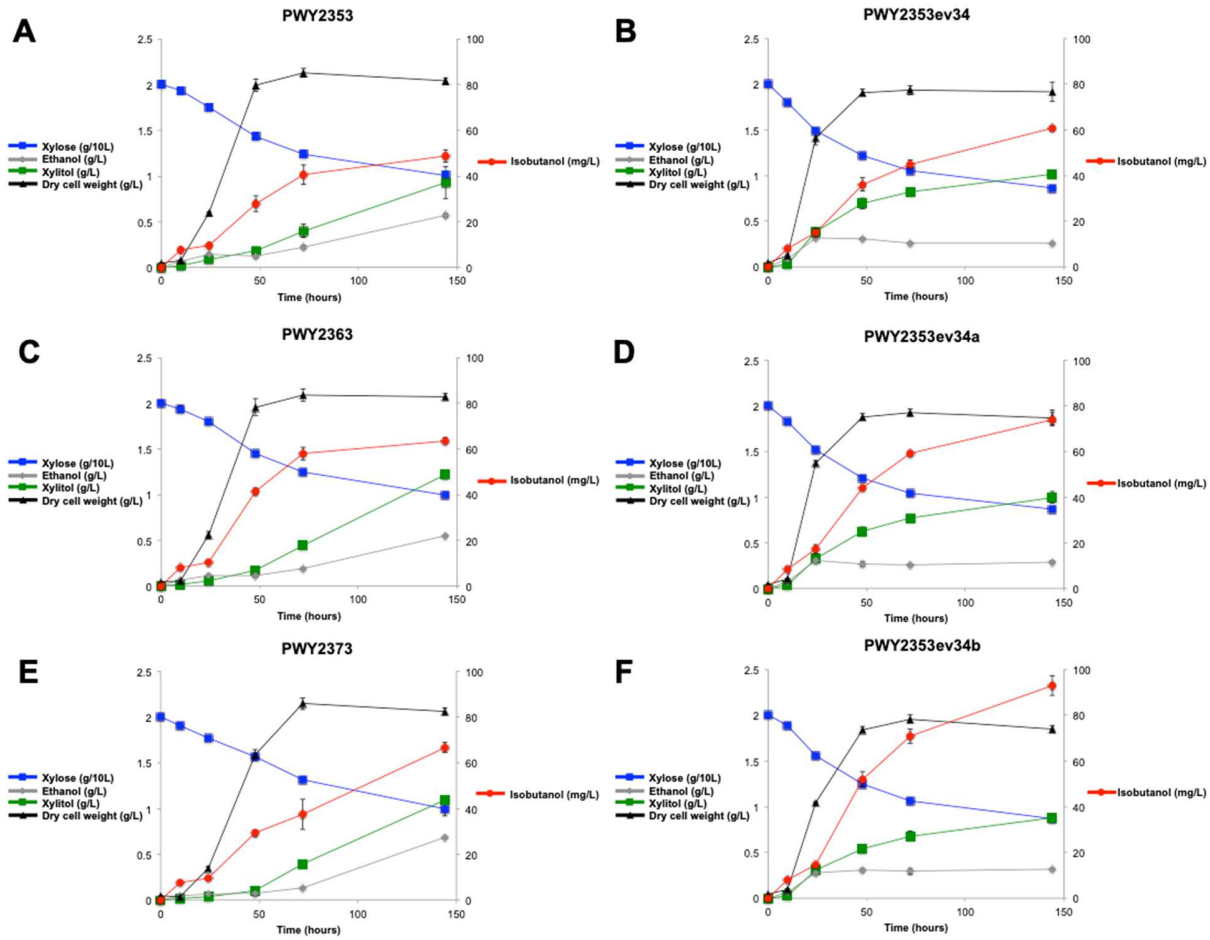

Figure 9. Strain improvement by integrating an additional copy of isobutanol pathway genes. Fermentation of strains PWY2353 (A). Fermentation of the evolved strain PWY2353ev34 (B). Fermentation of PWY2363, which contains one additional copy each of isobutanol pathway genes *LlkivD* and *ScADH7* (C). Fermentation of PWY2353ev34a, which is the evolved strain PWY2353ev34 that has one additional copy each of isobutanol pathway genes *LlkivD* and *ScADH7* (D). Fermentation of PWY2373, which contains one additional copy each of isobutanol pathway genes *LlkivD, ScADH7*, *ScIlv2*, *ScIlv5* and *ScIlv3* (E). Fermentation of PWY2353ev34b, which is the evolved strain PWY2353ev34 that has one additional copy each of isobutanol pathway genes *LlkivD, ScADH7*, *ScIlv2*, *ScIlv5* and *ScIlv3* (F). Concentration of xylose was plotted on the left, divided by 10, such that the maximum value of 2.5 on the scale indicates 25 g/L of xylose.

In order to verify that the increase in isobutanol production correlated with increased expression levels of the L-valine pathway genes and the keto-acid degradation pathway genes, we performed RT-PCR in the four engineered strains, PWY2363, PWY2373, PWY2353ev34a and PWY2353ev34a, as well as the parental strains PWY2353 and PWY2353ev34 (**Figure 10**). The expression levels of *Ll*kivD and *Sc*ADH7 were higher in strains PWY2363 and PWY2353ev34a, both of which have an additional copy each of the two genes integrated into the genome, compared to the levels observed in their corresponding parental strains (**Figure 10A** and **10B**). Similarly, the expression levels of *Sc*Ilv2, *Sc*Ilv5 and *Sc*Ilv3 were higher in strains PWY2373 and PWY2353ev34b, both of which have an additional copy each of the three genes integrated into the genome, when compared to the levels observed in their corresponding parental strains (**Figure 10C** and **10D**). As a control, the expression level of the acetyl-O-acyltransferase gene *Sc*ATF1 remained relatively unchanged between the engineered strains and their corresponding parental strains (**Figure 10E** and **10F)**.

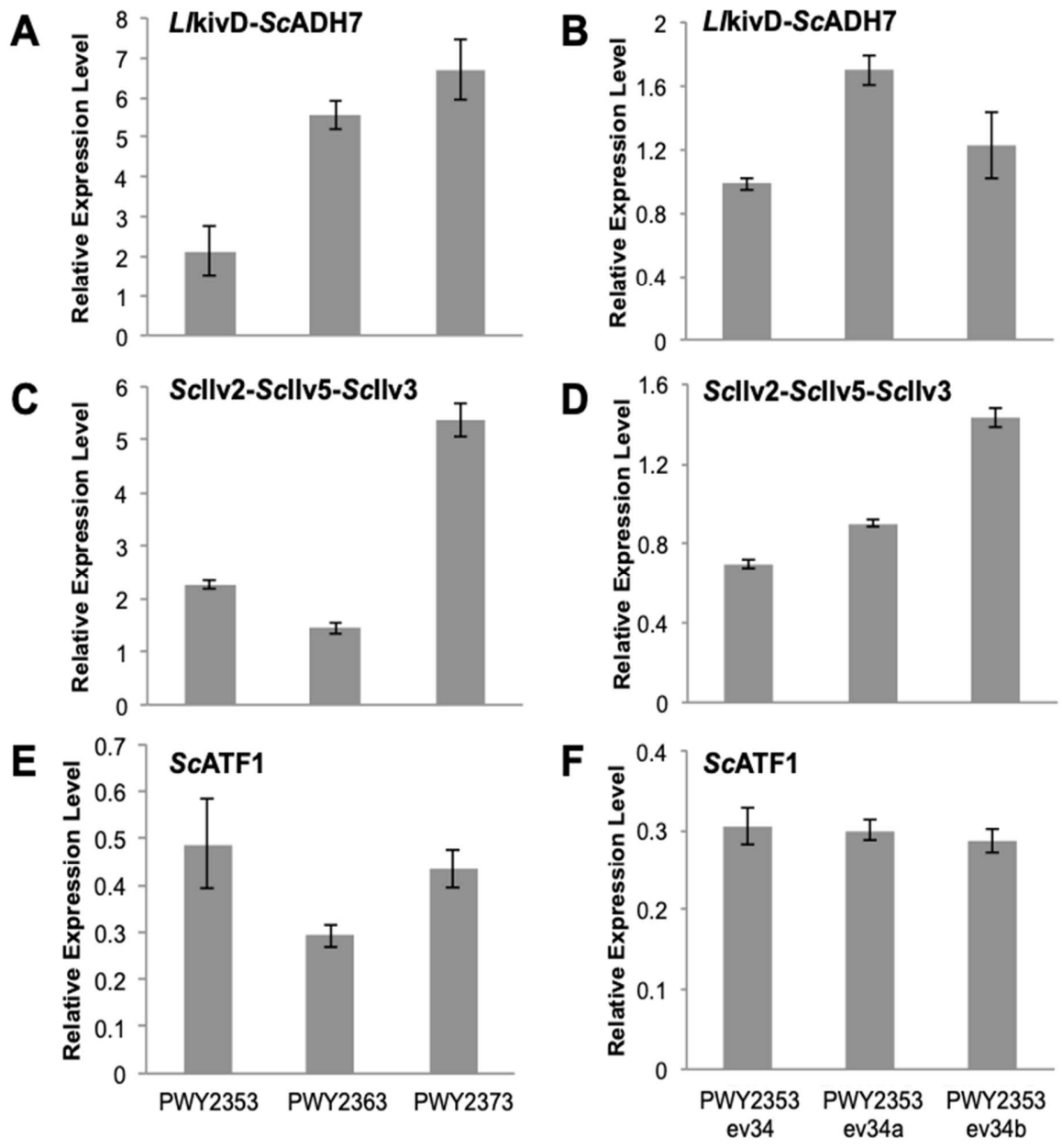

Figure 10. RT-PCR analysis of isobutanol biosynthetic pathway genes including *Ll*kivD-*Sc*ADH7 (A and B), *Sc*Ilv2-*Sc*Ilv5-*Sc*Ilv3 (C and D) and the alcohol *O*-acyltransferase gene *Sc*ATF1 (E and F) in engineered yeast strains.

4. Conclusions

In this work, we engineered the yeast *S. cerevisiae* to produce the biofuel isobutanol directly from D-xylose. Our strategy involved the expression of the xylose-specific sugar transporter to enable transport of D-xylose into the cell; the overexpression of xylulokinase from *S. stipitis* to convert D-xylulose to D-xylulose-5-phosphate, an intermediate in the pentose phosphate pathway (PPP); overexpression of an optimal XR-XDH combination; overexpression of the mitochondria-targeted isobutanol pathway enzymes; and deletion of the endogenous aldose reductase gene *GRE3* and the alkaline phosphatase gene *PHO13*. Further fine-tuning of the individual pathway gene led to an engineered strain that is able to produce 48.4 ± 2.0 mg/L (yield of 7.0 mg/g D-xylose). Next, we improved the yeast *Saccharomyces cerevisiae*'s ability to utilize D-xylose, and produce the advanced biofuel isobutanol by using a combination of adaptive laboratory engineering and rational metabolic engineering. Through the former strategy, we identified two single point mutations that improved yeast's growth on D-xylose: a single point-mutation in *CC4,* which encodes a subunit of the core CCR4-NOT complex that performs crucial roles in several cellular pathways and a single point mutation in *TIF1*, which encodes a subunit of the translation initiation factor 4F complex required for protein translation. Importantly, neither one of these genes has previously been implicated in the yeast's ability to utilize D-xylose. Reverse engineering of the parental, non-evolved strain with the two mutations improved the yeast's specific growth by 23% and 14%, respectively. Finally, using rational metabolic engineering, we fine-tuned the expression levels of the bottleneck enzymes in the isobutanol pathway and further improved the evolved strain's isobutanol titer to 92.9 ± 4.4 mg/L (specific isobutanol production of 50.2 ± 2.6 mg/g DCW). This is a 90% improvement in titer and a 110% improvement in specific production over the non-evolved strain. While these values are lower in comparison with glucose-based isobutanol production systems, given that xylose comprises a significant portion of biomass, we hope that our work will pave the way for an economic route to the advanced biofuel isobutanol and enable efficient utilization of xylose-containing biomass.

Acknowledgement

This work conducted by the National Center for Genetic Engineering and Biotechnology was supported by the Thailand Research Fund (TRF) under Contract No. TRG6180006.

References

1. Peralta-Yahya PP, Zhang F, del Cardayre SB, Keasling JD (2012) Microbial engineering for the production of advanced biofuels. Nature 488:320–8. https://doi.org/10.1038/nature11478
2. Kung Y, Runguphan W, Keasling JD (2012) From fields to fuels: recent advances in the microbial production of biofuels. ACS Synth Biol 1:498–513. https://doi.org/10.1021/sb300074k
3. Lee JW, Na D, Park JM, et al (2012) Systems metabolic engineering of microorganisms for natural and non-natural chemicals. Nat. Chem. Biol. 8:536–546
4. Peralta-Yahya PP, Ouellet M, Chan R, et al (2011) Identification and microbial production of a terpene-based advanced biofuel. Nat Commun 2:483. https://doi.org/10.1038/ncomms1494
5. Atsumi S, Hanai T, Liao JC (2008) Non-fermentative pathways for synthesis of branched-chain higher alcohols as biofuels. Nature 451:86–89. https://doi.org/10.1038/nature06450
6. Choi YJ, Lee SY (2013) Microbial production of short-chain alkanes. Nature 502:571–4. https://doi.org/10.1038/nature12536
7. Buijs NA, Zhou YJ, Siewers V, Nielsen J (2015) Long-chain alkane production by the yeast Saccharomyces cerevisiae. Biotechnol Bioeng 112:1275–1279. https://doi.org/10.1002/bit.25522
8. Steen EJ, Kang Y, Bokinsky G, et al (2010) Microbial production of fatty-acid-derived fuels and chemicals from plant biomass. Nature 463:559–562. https://doi.org/10.1038/nature08721
9. Runguphan W, Keasling JD (2013) Metabolic engineering of Saccharomyces cerevisiae for production of fatty acid-derived biofuels and chemicals. Metab Eng 1–11. https://doi.org/10.1016/j.ymben.2013.07.003
10. Dellomonaco C, Clomburg JM, Miller EN, Gonzalez R (2011) Engineered reversal of the β-oxidation cycle for the synthesis of fuels and chemicals. Nature 476:355–359.

https://doi.org/10.1038/nature10333
11. Kwak S, Jin YS (2017) Production of fuels and chemicals from xylose by engineered Saccharomyces cerevisiae: A review and perspective. Microb. Cell Fact. 16:82
12. Mosier N, Wyman C, Dale B, et al (2005) Features of promising technologies for pretreatment of lignocellulosic biomass. Bioresour Technol 96:673–686. https://doi.org/10.1016/j.biortech.2004.06.025
13. Li X, Chen Y, Nielsen J (2019) Harnessing xylose pathways for biofuels production. Curr. Opin. Biotechnol. 57:56–65
14. Zhang B, Sun H, Li J, et al (2016) High-titer-ethanol production from cellulosic hydrolysate by an engineered strain of Saccharomyces cerevisiae during an in situ removal process reducing the inhibition of ethanol on xylose metabolism. Process Biochem 51:967–972. https://doi.org/10.1016/j.procbio.2016.04.019
15. Moysés DN, Reis VCB, de Almeida JRM, et al (2016) Xylose fermentation by saccharomyces cerevisiae: Challenges and prospects. Int. J. Mol. Sci. 17:207
16. Generoso WC, Schadeweg V, Oreb M, Boles E (2015) Metabolic engineering of Saccharomyces cerevisiae for production of butanol isomers. Curr. Opin. Biotechnol. 33:1–7
17. Lamsen EN, Atsumi S (2012) Recent progress in synthetic biology for microbial production of C3-C10 alcohols. Front Microbiol 3:196. https://doi.org/10.3389/fmicb.2012.00196
18. Atsumi S, Higashide W, Liao JC (2009) Direct photosynthetic recycling of carbon dioxide to isobutyraldehyde. Nat Biotechnol 27:1177–1180. https://doi.org/10.1038/nbt.1586
19. Lu J, Brigham CJ, Gai CS, Sinskey AJ (2012) Studies on the production of branched-chain alcohols in engineered Ralstonia eutropha. Appl Microbiol Biotechnol 96:283–297. https://doi.org/10.1007/s00253-012-4320-9
20. Siripong W, Wolf P, Kusumoputri TP, et al (2018) Metabolic engineering of Pichia pastoris for production of isobutanol and isobutyl acetate. Biotechnol Biofuels 11:1. https://doi.org/10.1186/s13068-017-1003-x
21. Brat D, Boles E (2013) Isobutanol production from d-xylose by recombinant Saccharomyces cerevisiae. FEMS Yeast Res 13:241–244. https://doi.org/10.1111/1567-1364.12028

22. Matsuda F, Ishii J, Kondo T, et al (2013) Increased isobutanol production in Saccharomyces cerevisiae by eliminating competing pathways and resolving cofactor imbalance. Microb Cell Fact 12:119. https://doi.org/10.1186/1475-2859-12-119
23. Chee MK, Haase SB (2012) New and redesigned pRS plasmid shuttle vectors for genetic manipulation of saccharomyces cerevisiae. G3 Genes, Genomes, Genet 2:515–526. https://doi.org/10.1534/g3.111.001917
24. Schneider JC, Guarente L (1991) Vectors for Expression of Cloned Genes in Yeast: Regulation, Overproduction, and Underproduction. Methods Enzymol 194:373–388. https://doi.org/10.1016/0076-6879(91)94028-B
25. Farzadfard F, Perli SD, Lu TK (2013) Tunable and Multifunctional Eukaryotic Transcription Factors Based on CRISPR/Cas. ACS Synth Biol 2:604–613. https://doi.org/10.1021/sb400081r
26. DiCarlo JE, Norville JE, Mali P, et al (2013) Genome engineering in Saccharomyces cerevisiae using CRISPR-Cas systems. Nucleic Acids Res 41:4336–43. https://doi.org/10.1093/nar/gkt135
27. Reider Apel A, d'Espaux L, Wehrs M, et al (2016) A Cas9-based toolkit to program gene expression in Saccharomyces cerevisiae. Nucleic Acids Res 45:496–508. https://doi.org/10.1093/nar/gkw1023
28. Gueldener U, Heinisch J, Koehler GJ, et al (2002) A second set of loxP marker cassettes for Cre-mediated multiple gene knockouts in budding yeast. Nucleic Acids Res 30:e23–e23. https://doi.org/10.1093/nar/30.6.e23
29. Gietz RD, Schiestl RH (2007) Frozen competent yeast cells that can be transformed with high efficiency using the LiAc/SS carrier DNA/PEG method. Nat Protoc 2:1–4. https://doi.org/10.1038/nprot.2007.17
30. Gietz RD, Schiestl RH (2007) High-efficiency yeast transformation using the LiAc/SS carrier DNA/PEG method. Nat Protoc 2:31–34. https://doi.org/10.1038/nprot.2007.13
31. Hegemann JH, Heick SB (2011) Strain Engineering: Delete and Repeat--a comprehensive toolkit for sequential gene knockout in the budding yeast S. cerevisiae. Strain Eng Methods Protoc 765:. https://doi.org/10.1007/978-1-61779-197-0
32. Boeke JD, La Croute F, Fink GR (1984) A positive selection for mutants lacking orotidine-5′-

phosphate decarboxylase activity in yeast: 5-fluoro-orotic acid resistance. MGG Mol Gen Genet 197:345–346. https://doi.org/10.1007/BF00330984

33. Chen S, Zhou Y, Chen Y, Gu J (2018) fastp: an ultra-fast all-in-one FASTQ preprocessor. Bioinformatics 34:i884–i890. https://doi.org/10.1093/bioinformatics/bty560
34. Li H, Durbin R (2009) Fast and accurate short read alignment with Burrows–Wheeler transform. Bioinformatics 25:1754–1760. https://doi.org/10.1093/bioinformatics/btp324
35. McKenna A, Hanna M, Banks E, et al (2010) The genome analysis toolkit: A MapReduce framework for analyzing next-generation DNA sequencing data. Genome Res 20:1297–1303. https://doi.org/10.1101/gr.107524.110
36. Promdonkoy P, Siripong W, Downes JJ, et al (2019) Systematic improvement of isobutanol production from d-xylose in engineered Saccharomyces cerevisiae. AMB Express 9:160. https://doi.org/10.1186/s13568-019-0885-3
37. Cam Y, Alkim C, Trichez D, et al (2016) Engineering of a Synthetic Metabolic Pathway for the Assimilation of (d)-Xylose into Value-Added Chemicals. ACS Synth Biol 5:607–618. https://doi.org/10.1021/acssynbio.5b00103
38. Chomvong K, Bauer S, Benjamin DI, et al (2016) Bypassing the pentose phosphate pathway: Towards modular utilization of xylose. PLoS One 11:e0158111. https://doi.org/10.1371/journal.pone.0158111
39. AV Sarthy BMZLJSCFBH (1987) Expression of the Escherichia coli xylose isomerase gene in Saccharomyces cerevisiae. Appl Env Microbiol 53:1996–2000
40. Amore R, Wilhelm M, Hollenberg CP (1989) The fermentation of xylose -an analysis of the expression of Bacillus and Actinoplanes xylose isomerase genes in yeast. Appl Microbiol Biotechnol 30:351–357. https://doi.org/10.1007/BF00296623
41. Moes CJ, Pretorius IS, Van Zyl WH (1996) Cloning and expression of the clostridium thermosulfurogenes d-xylose isomerase gene (xylA) in saccharomyces cerevlsiae. Biotechnol Lett 18:269–274. https://doi.org/10.1007/BF00142943
42. Apel AR, Ouellet M, Szmidt-Middleton H, et al (2016) Evolved hexose transporter enhances xylose uptake and glucose/xylose co-utilization in Saccharomyces cerevisiae. Sci Rep 6:19512. https://doi.org/10.1038/srep19512
43. Parreiras LS, Breuer RJ, Narasimhan RA, et al (2014) Engineering and two-stage evolution

of a lignocellulosic hydrolysate-tolerant Saccharomyces cerevisiae strain for anaerobic fermentation of xylose from AFEX pretreated corn stover. PLoS One 9:e107499. https://doi.org/10.1371/journal.pone.0107499

44. Xu H, Kim S, Sorek H, et al (2016) PHO13 deletion-induced transcriptional activation prevents sedoheptulose accumulation during xylose metabolism in engineered Saccharomyces cerevisiae. Metab Eng 34:88–96. https://doi.org/10.1016/j.ymben.2015.12.007
45. Johansson B, Christensson C, Hobley T, Hahn-Hägerdal B (2001) Xylulokinase Overexpression in Two Strains of Saccharomyces cerevisiae Also Expressing Xylose Reductase and Xylitol Dehydrogenase and Its Effect on Fermentation of Xylose and Lignocellulosic Hydrolysate. Appl Environ Microbiol 67:4249–4255. https://doi.org/10.1128/AEM.67.9.4249-4255.2001
46. Kim SR, Skerker JM, Kang W, et al (2013) Rational and Evolutionary Engineering Approaches Uncover a Small Set of Genetic Changes Efficient for Rapid Xylose Fermentation in Saccharomyces cerevisiae. PLoS One 8:e57048. https://doi.org/10.1371/journal.pone.0057048
47. Guo W, Sheng J, Zhao H, Feng X (2016) Metabolic engineering of Saccharomyces cerevisiae to produce 1-hexadecanol from xylose. Microb Cell Fact 15:24. https://doi.org/10.1186/s12934-016-0423-9
48. Li X, Park A, Estrela R, et al (2016) Comparison of xylose fermentation by two high-performance engineered strains of Saccharomyces cerevisiae. Biotechnol Reports 9:53–56. https://doi.org/10.1016/j.btre.2016.01.003
49. C Baker Brachmann ADGCECJLPHJB (1998) Designer deletion strains derived from Saccharomyces cerevisiae S288C: a useful set of strains and plasmids for PCR-mediated gene disruption and other applications. Yeast 14:115–132. https://doi.org/10.1002/(sici)1097-0061(19980130)14:2<115::aid-yea204>3.0.co
50. DeRisi JL, Iyer VR, Brown PO (1997) Exploring the metabolic and genetic control of gene expression on a genomic scale. Science (80-) 278:680–686. https://doi.org/10.1126/science.278.5338.680
51. Egner A, Jakobs S, Hell SW (2002) Fast 100-nm resolution three-dimensional microscope

reveals structural plasticity of mitochondria in live yeast. Proc Natl Acad Sci U S A 99:3370–3375. https://doi.org/10.1073/pnas.052545099

52. José L. Avalos; Gerald R. Fink; and Gregory Stephanopoulos (2013) Compartmentalization of metabolic pathways in yeast mitochondria improves production of branched chain alcohols. Nat Biotechnol 31:335–341. https://doi.org/10.1038/nbt.2509.Compartmentalization
53. Ryan MD, Drew J (1994) Foot-and-mouth disease virus 2A oligopeptide mediated cleavage of an artificial polyprotein. EMBO J 13:928–933. https://doi.org/10.1002/j.1460-2075.1994.tb06337.x
54. Karhumaa K, Sanchez RG, Hahn-Hägerdal B, Gorwa-Grauslund MF (2007) Comparison of the xylose reductase-xylitol dehydrogenase and the xylose isomerase pathways for xylose fermentation by recombinant Saccharomyces cerevisiae. Microb Cell Fact 6:5. https://doi.org/10.1186/1475-2859-6-5
55. Ehrensberger AH, Elling RA, Wilson DK (2006) Structure-guided engineering of xylitol dehydrogenase cosubstrate specificity. Structure 14:567–575. https://doi.org/10.1016/j.str.2005.11.016
56. Watanabe S, Saleh AA, Pack SP, et al (2007) Ethanol production from xylose by recombinant Saccharomyces cerevisiae expressing protein engineered NADP+-dependent xylitol dehydrogenase. J Biotechnol 130:316–319. https://doi.org/10.1016/j.jbiotec.2007.04.019
57. Baek SH, Kwon EY, Bae SJ, et al (2017) Improvement of d-Lactic Acid Production in Saccharomyces cerevisiae Under Acidic Conditions by Evolutionary and Rational Metabolic Engineering. Biotechnol J 12:1700015. https://doi.org/10.1002/biot.201700015
58. Dragosits M, Mattanovich D (2013) Adaptive laboratory evolution – principles and applications for biotechnology. Microb Cell Fact 12:64. https://doi.org/10.1186/1475-2859-12-64
59. Caspeta L, Chen Y, Ghiaci P, et al (2014) Altered sterol composition renders yeast thermotolerant. Science (80-) 346:75 LP – 78. https://doi.org/10.1126/science.1258137
60. van Maris AJA, Geertman J-MA, Vermeulen A, et al (2004) Directed evolution of pyruvate decarboxylase-negative Saccharomyces cerevisiae, yielding a C2-independent, glucose-

tolerant, and pyruvate-hyperproducing yeast. Appl Environ Microbiol 70:159–166. https://doi.org/10.1128/aem.70.1.159-166.2004

61. Davis López SA, Griffith DA, Choi B, et al (2018) Evolutionary engineering improves tolerance for medium-chain alcohols in Saccharomyces cerevisiae. Biotechnol Biofuels 11:90. https://doi.org/10.1186/s13068-018-1089-9
62. Collart MA, Panasenko OO (2012) The Ccr4–Not complex. Gene 492:42–53. https://doi.org/https://doi.org/10.1016/j.gene.2011.09.033
63. Miller JE, Reese JC (2012) Ccr4-Not complex: the control freak of eukaryotic cells. Crit Rev Biochem Mol Biol 47:315–333. https://doi.org/10.3109/10409238.2012.667214
64. Traven A, Hammet A, Tenis N, et al (2005) Ccr4-not complex mRNA deadenylase activity contributes to DNA damage responses in Saccharomyces cerevisiae. Genetics 169:65–75. https://doi.org/10.1534/genetics.104.030940
65. Lenssen E, James N, Pedruzzi I, et al (2005) The Ccr4-Not complex independently controls both Msn2-dependent transcriptional activation--via a newly identified Glc7/Bud14 type I protein phosphatase module--and TFIID promoter distribution. Mol Cell Biol 25:488–498. https://doi.org/10.1128/MCB.25.1.488-498.2005
66. Azzouz N, Panasenko OO, Deluen C, et al (2009) Specific roles for the Ccr4-Not complex subunits in expression of the genome. RNA 15:377–383. https://doi.org/10.1261/rna.1348209
67. Cui Y, Ramnarain DB, Chiang Y-C, et al (2008) Genome wide expression analysis of the CCR4-NOT complex indicates that it consists of three modules with the NOT module controlling SAGA-responsive genes. Mol Genet Genomics 279:323–337. https://doi.org/10.1007/s00438-007-0314-1
68. Li Q, Imataka H, Morino S, et al (1999) Eukaryotic translation initiation factor 4AIII (eIF4AIII) is functionally distinct from eIF4AI and eIF4AII. Mol Cell Biol 19:7336–7346. https://doi.org/10.1128/mcb.19.11.7336
69. Gupta N, Lorsch JR, Hinnebusch AG (2018) Yeast Ded1 promotes 48S translation preinitiation complex assembly in an mRNA-specific and eIF4F-dependent manner. Elife 7:. https://doi.org/10.7554/eLife.38892
70. Schmid SR, Linder P (1991) Translation initiation factor 4A from Saccharomyces cerevisiae:

analysis of residues conserved in the D-E-A-D family of RNA helicases. Mol Cell Biol 11:3463–3471. https://doi.org/10.1128/mcb.11.7.3463

71. Basquin J, Roudko V V, Rode M, et al (2012) Architecture of the Nuclease Module of the Yeast Ccr4-Not Complex: the Not1-Caf1-Ccr4 Interaction. Mol Cell 48:207–218. https://doi.org/https://doi.org/10.1016/j.molcel.2012.08.014

72. Obenauer JC, Cantley LC, Yaffe MB (2003) Scansite 2.0: proteome-wide prediction of cell signaling interactions using short sequence motifs. Nucleic Acids Res 31:3635–3641. https://doi.org/10.1093/nar/gkg584

73. Blom N, Gammeltoft S, Brunak S (1999) Sequence and structure-based prediction of eukaryotic protein phosphorylation sites1 1Edited by F. E. Cohen. J Mol Biol 294:1351–1362. https://doi.org/https://doi.org/10.1006/jmbi.1999.3310

Supporting Information

Table S1. Primers used in this study. Nucleotides highlighted in red are the 20-bp spacer sequence that targets the gene on interest in CRISPR/Cas9-assisted genome editing; **bold** nucleotides designate the Kozak sequence; underlined nucleotides are restriction sites.

Name	Sequence (5' to 3')
GRE3-del-F	TAATATAAATCGTAAAGGAAAATTGGAAATTTTTTAAAGATGCATAGGCCACTAGTGGAT
GRE3-del-R	TGTTCATATCGTCGTTGAGTATGGATTTTACTGGCTGGATCACAGCTGAAGCTTCGTACG
PHO13-del-F	TTATAGCTTGCCCTGACAAAGAATATACAACTCGGGAAAATGCATAGGCCACTAGTGGAT
PHO13-del-R	TCAAAAAGTAATTCTACCCCTAGATTTTGCATTGCTCCTCTACAGCTGAAGCTTCGTACG
S1	ATAGGATCC**AAAACA**ATGACCACTACCCCATTTG
S2	ATAGAATTCTTAGTGTTTCAATTCACTTTCC
S3	GCAATCTAATCTAAGTTTTCTAGAACTAGTGGATCC**AAAACA**ATGTCACAAGACGCTGCT
S4	CCAGTATCCCAACCGGAAACGAAACCACCAAAGG
S5	TTGGTGGTTTCGTTTCCGGTTGGGATACTGGTAC
S6	GAGGTCGACGGTATCGATAAGCTTGATATCGAATTCTTATTTGGTGCTGAACATTCT
S7	ATAGGATCC**AAAACA**ATGTTTAAATTTTTCACTTCTC
S8	ATAGAATTCTTAAACAAAGATTGGAATGTTG
S9	ATAGGATCC**AAAACA**ATGCCTTCTATTAAGTTGAAC
S10	ATACCCGGGTTAGACGAAGATAGGAATCTT
S11	ATATATCCGCGG**AAAACA**ATGACTGCAAACCCATCA
S12	ATATATGAATTCCTATTCTGGACCATCAATTAAAC
S13	ATATATCCGCGG**AAAACA**ATGACTGCTAACCCTTCC

S14	ATATATGAATTCTTACTCAGGGCCGTCAAT
S15	ATACGACTCACTATAGGGAGACCGGCAGATCCGCGGGAGTTTATCATT
S16	AGTGTACATTGTTTTCCGCGGTTTGTTTGTTTA
S17	GGTTCTTTGTTGACTTGTGGAGATGTTGAGGAGAATCCAGGACCAATGCTTTACCCAGAAAAATTT
S18	GACGGTATCGATAAGCTTGATATCGAATTCCTATTTATGGAATTTCTTATCATA
S19	ACAAACAAACCGCGGAAAACAATGTACACTGTCGGA
S20	CTCAACATCTCCACAAGTCAACAAAGAACCCCTTCCTTCTGCTCTGGATTTGTTCTGTTCTGCGAA
S21	AAGTTCTTGTGGCTGGCTTGAAAAATCTTATAGATTGACGTAGTGAAAGCATTGTTTTCCGCGGTTT
S22	ATTTTTCAAGCCAGCCACAAGAACTTTGTGTAGCTCTAGATATCTGCTTTACACTGTCGGAGATTAC
S23	AGTTCTAGTAGCAGGCTTAAAGAAtCTTATAGATTGACGTAGTGAAAGCATTGGTCCTGGATTCTC
S24	ATTCTTTAAGCCTGCTACTAGAACTtTGTGTAGCTCTAGATATCTGCTTCTTTACCCAGAAAAATTTCAG
S25	CTTGCTCATTAGAAAGAAAGCATAGCAATCTAATCTAAGTTTTCTAGAACTAGTGGATCCAAAACAATGATCA GACAATCTACGCTA
S26	TGGTCCTGGATTCTCCTCAACATCTCCACAAGTCAACAAAGAACCCCTTCCTTCTGCTCTGTGCTTACCGCCTGTACG
S27	AGAGCAGAAGGAAGGGGTTCTTTGTTGACTTGTGGAGATGTTGAGGAGAATCCAGGACCATTGAGAACTCAAGCCGCC
S28	AGGACCAGGGTTTTCTTCTACGTCACCGCATGTTAGTAGACTTCCTCTACCCTCAGCTCTTTGGTTTTCTGGTCTCAACTT
S29	AGAGCTGAGGGTAGAGGAAGTCTACTAACATGCGGTGACGTAGAAGAAAACCCTGGTCCTGGCTTGTTAACGAAAGTTGCT
S30	GTGACATAACTAATTACATGACTCGAGGTCGACGGTATCGATAAGCTTGATATCGAATTCTCAAGCATCTAAAACACAACC

S31	ATATGGGCCCGAGTTTATCATTATCAATACTGCC
S32	ATATCCCGGGGGCCGCAAATTAAAGCCT
S33	ATATATGCGGCCGCATAGCTTCAAAATGTTTCTACTC
S34	ATATATGAGCTCGGCCGCAAATTAAAGCCT
S35	ATATATCTGCAGATAGCTTCAAAATGTTTCTACTC
S36	ATATATGCGGCCGCGGCCGCAAATTAAAGCCT
S37	ATATATGCGGCCGCGAGTTTATCATTATCAATACTGCC
ARS208intF	AGGGACCATACACACGTCCGCTAAACAAAAGATCTTGGGCATCAGCTGAAGCTTCGTACG
ARS208intR	CCCTCTTTTCCACCCCGTGAAAAACAGAATATCATTAACCGGACGACTCACTATAGGGCG
YMRWΔ15intF	GATGACTGTTTCTCAAACTTTATGTCATTTTCTTACACCGCACAGCTGAAGCTTCGTACG
YMRWΔ15intR	ACCGCGAAGATTTATAATGGTTTATCGGTTGCATTTTCCATGACGACTCACTATAGGGCG
ARS308intF	GAAATTTCAACATTAACTTCGAATTTTTTTCTTTTTATCTAACAGCTGAAGCTTCGTACG
ARS308intR	TAGAAGTGGTAGCAATATGTAGCAAAGAAGACAAGTAATCCTACGACTCACTATAGGGCG
ARS720intF	GTTACTGTTGATTGTTCGTTTATTTGTATAATTGAGTTTACACAGCTGAAGCTTCGTACG
ARS720intR	ATTTATAAGTTTGCTTTTTGTCACTCTCTTGGCCCTAATTACACGACTCACTATAGGGCG
ARS1309intF	ATTCTAGTATCAAAGAAACTTACTATGACGCAGTTTAGGATCCAGCTGAAGCTTCGTACG
ARS1309intR	ACACTGAATAAACAAGGGGCTTTACGATGGAGTAGTAGACCTACGACTCACTATAGGGCG
YORWΔ22intF	CACCGGAGCTTGGATATGATAAACGAAATATTCTTGAATCGTCCGCGGGAGTTTATCATT
YORWΔ22intR	CGTGATAAACGATCGCCATAACTAACAGGTATAAATGGCAGCAAGCTTCGTACGCTGCAG
HIS3-hom-F	TAACGCGAATTTTAACAAAATATTAACGTTTACAATTTCGAGTTCAAGAGAAAAAAAAAG
HIS3-hom-R	ACTATGCGGCATCAGAGCAGATTGTACTGAGAGTGCACCATACGTTTTAAGAGCTTGGTG

CCR4_gRNA_F	ATAAAGCTTAAGCTACAACACATTCCTAGGTTTTAGAGCTAGAAATAGCA
univl_gRNA_R	ATACTCGAGAAAAAAGCACCG
TIF1_gRNA_F	ATAAAGCTTGCACGTTGTTGAATGGCAGAGTTTTAGAGCTAGAAATAGCA
CCR4_seq_F	GTAGGTTCATCGAAATCAATAC
CCR4_don_R1	CATATGGTGTCGCCAGATGGAATGTGTTGTAGC
CCR4_don_F2	GCTACAACACATTCCATCTGGCGACACCATATG
CCR4_seq_R	CTCACGTATTCAGGGTCC
TIF1_seq_F	GGTTTATCAGCAACAACATC
TIF1_don_R1	ACGTTGTTGAATGGCGCTTGGTTCTTCGAAACC
TIF1_don_F2	GGTTTCGAAGAACCAAGCGCCATTCAACAACGT
TIF1_seq_R	CACTCGTATTTGTATTCTTCTTC
ARS416_int_F	ATGCGAGATCCGTTTAACCGGACCCTAGTGCACTTACCCCACATAGGGAGACCGGCAGAT
ARS416_int_R	TAAAATAGTGAAGGAGCATGTTCGGCACACAGTGGACCGAACCAGCTGAAGCTTCGTACG
ARS416_ups_F	CCTCATCAATGCGAGATCCG
ARS416_dws_R	GTGAAGGAGCATGTTCGGC
ARS1014_int_F	ATTTCATGATAGTGCATCAAGAGACCCTAAAATTAATATCCTCAGCTGAAGCTTCGTACG
ARS1014_int_R	ACCGTCCCACGTCTAGATGAAAACAGTGATAATTTACTACCAACGACTCACTATAGGGCG
ARS1014_ups_F	CCTTAACAACAATGGAATACG
ARS1014_dws_R	CGAAAATGTTACCGTCCC
ScTAF10_RT_F	GCGAGAGCTAGGCAGCTATT
ScTAF10_RT_R	ATCGTTCACCGTCAGAACAA

ScIlv2-ScIlv5-ScIlv3_RT_F	CGGTAAGCACAGAGCAGAAG
ScIlv2-ScIlv5-ScIlv3_RT_R	GCCAAAGCAAAGGTTCTCTTA
LlkivD-ScADH7_RT_F	TCGCAGAACAGAACAAATCC
LlkivD-ScADH7_RT_R	AAATACCGATGCCCTGAAAT
ScATF1_RT_F	AGCATCTCCATGGCTTAGGG
ScATF1_RT_R	ATATTTGGCATCGGGCTCCT

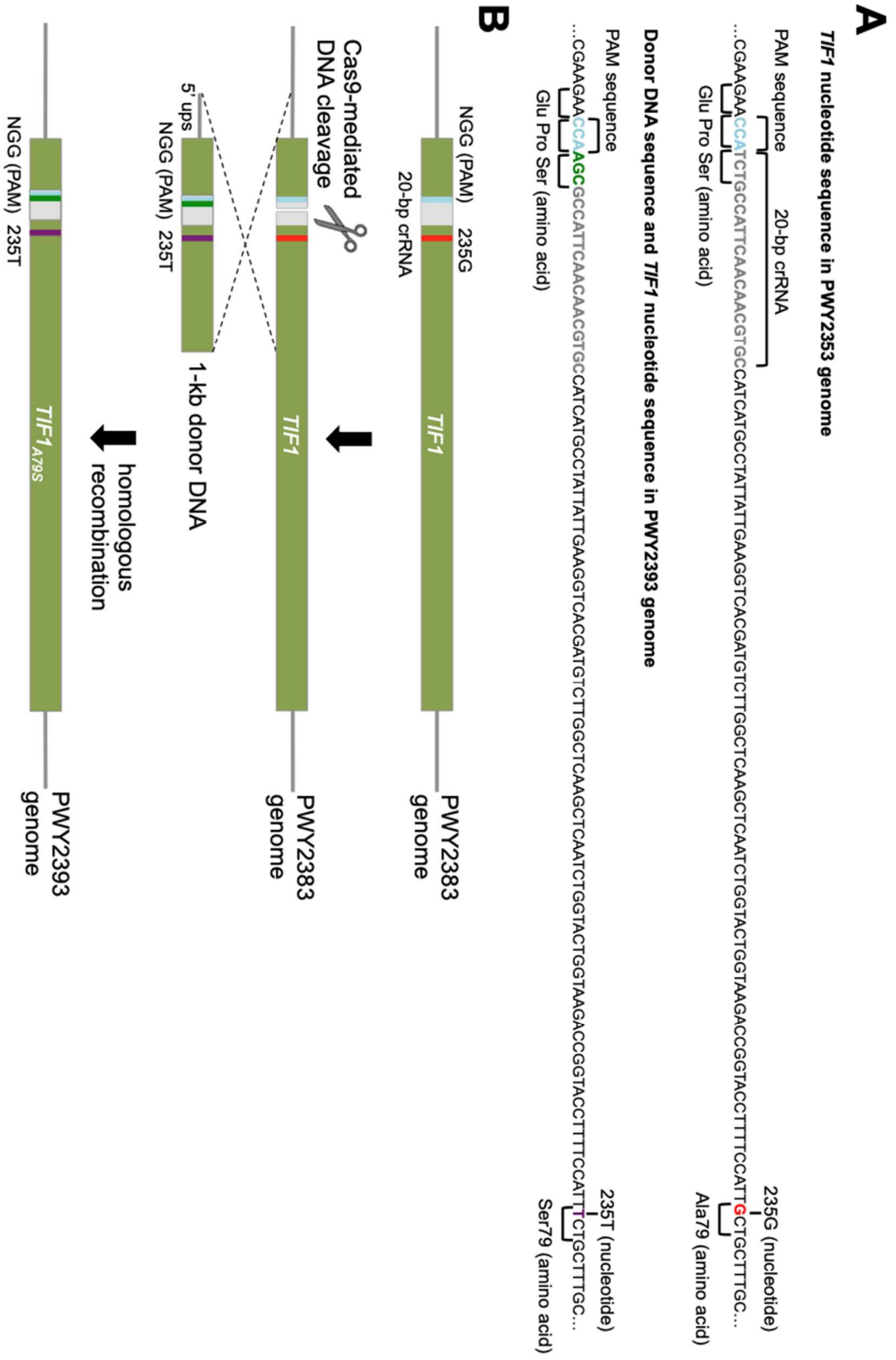

Figure S1.

Strategy to reverse engineer PWY2383 with *TIF1*$_{A79S}$ to create strain PWY2393

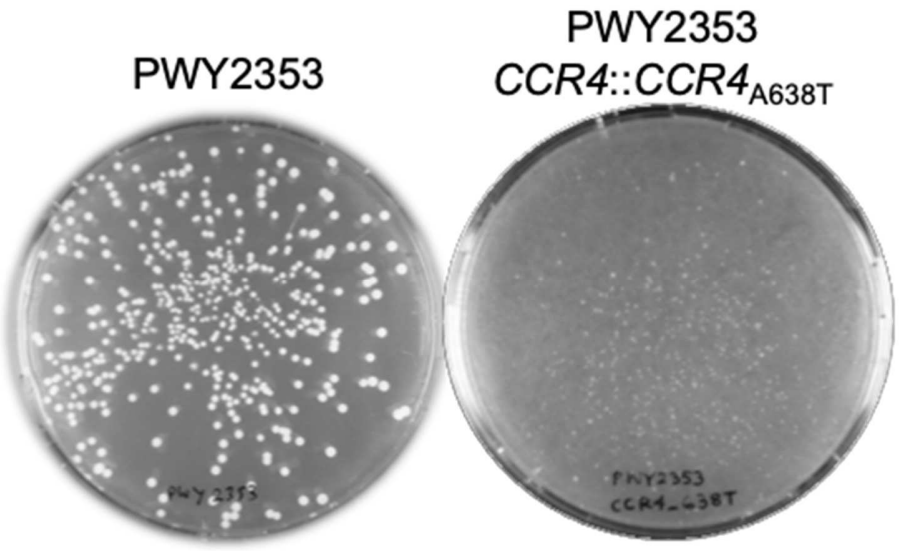

Figure S2. Colony characteristics of engineered *S. cerevisiae* strain PWY2353 (left) and PWY2353 $CCR4_{A638T}$ (Right). The plates were incubated at 30 °C for 72 hours.